NASA/TM—2017–219111

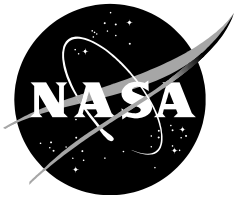

Wheels-off Time Uncertainty Impact on Benefits of Early Call For Release Scheduling

Kee Palopo
Ames Research Center
Moffett Field, California

Gano B. Chatterji
University of California Santa Cruz
Moffett Field, California

Noam Almog
Aerospace Computing Inc.
Moffett Field, California

June 2017

NASA STI Program ... in Profile

Since its founding, NASA has been dedicated to the advancement of aeronautics and space science. The NASA scientific and technical information (STI) program plays a key part in helping NASA maintain this important role.

The NASA STI program operates under the auspices of the Agency Chief Information Officer. It collects, organizes, provides for archiving, and disseminates NASA's STI. The NASA STI program provides access to the NTRS Registered and its public interface, the NASA Technical Reports Server, thus providing one of the largest collections of aeronautical and space science STI in the world. Results are published in both non-NASA channels and by NASA in the NASA STI Report Series, which includes the following report types:

- TECHNICAL PUBLICATION. Reports of completed research or a major significant phase of research that present the results of NASA Programs and include extensive data or theoretical analysis. Includes compilations of significant scientific and technical data and information deemed to be of continuing reference value. NASA counterpart of peer-reviewed formal professional papers but has less stringent limitations on manuscript length and extent of graphic presentations.

- TECHNICAL MEMORANDUM. Scientific and technical findings that are preliminary or of specialized interest, e.g., quick release reports, working papers, and bibliographies that contain minimal annotation. Does not contain extensive analysis.

- CONTRACTOR REPORT. Scientific and technical findings by NASA-sponsored contractors and grantees.

- CONFERENCE PUBLICATION. Collected papers from scientific and technical conferences, symposia, seminars, or other meetings sponsored or co-sponsored by NASA.

- SPECIAL PUBLICATION. Scientific, technical, or historical information from NASA programs, projects, and missions, often concerned with subjects having substantial public interest.

- TECHNICAL TRANSLATION. English-language translations of foreign scientific and technical material pertinent to NASA's mission.

Specialized services also include organizing and publishing research results, distributing specialized research announcements and feeds, providing information desk and personal search support, and enabling data exchange services.

For more information about the NASA STI program, see the following:

- Access the NASA STI program home page at http://www.sti.nasa.gov

- E-mail your question to help@sti.nasa.gov

- Phone the NASA STI Information Desk at 757-864-9658

- Write to:
  NASA STI Information Desk
  Mail Stop 148
  NASA Langley Research Center
  Hampton, VA 23681-2199

NASA/TM—2017–219111

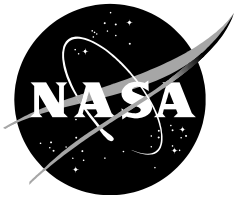

Wheels-off Time Uncertainty Impact on Benefits of Early Call For Release Scheduling

Kee Palopo
Ames Research Center
Moffett Field, California

Gano B. Chatterji
University of California Santa Cruz
Moffett Field, California

Noam Almog
Aerospace Computing Inc.
Moffett Field, California

National Aeronautics and
Space Administration

Ames Research Center
Moffett Field, California 94035-1000

June 2017

Available from:

NASA Center for AeroSpace Information
7115 Standard Drive
Hanover, MD 21076-1320
443-757-5802

This report is also available in electronic form at

https://ntrs.nasa.gov

TABLE OF CONTENTS

LIST OF FIGURES

LIST OF TABLES

WHEELS-OFF TIME UNCERTAINTY IMPACT ON BENEFITS OF EARLY CALL FOR RELEASE SCHEDULING

Kee Palopo
Ames Research Center

Gano B. Chatterji
University of California Santa Cruz

Noam Almog
Aerospace Computing Inc.

ABSTRACT

Arrival traffic scenarios with 808 flights from 173 airports to Houston George Bush International airport are simulated to determine if Call For Release flights can receive a benefit in terms of less delay over other flights by scheduling prior to gate pushback (look-ahead in time) as opposed to at gate pushback. Call for Release flights are departures that require approval from Air Route Traffic Control Center prior to release. Realism is brought to the study by including gate departure delay and taxi-out delay uncertainties for the 77 major U. S. airports. Gate departure delay uncertainty is assumed to increase as a function of look-ahead time. Results show that Call For Release flights from an airport within the freeze horizon (a region surrounding the arrival airport) can get an advantage over other flights to a capacity constrained airport by scheduling prior to gate pushback, provided the wheels-off time uncertainty with respect to schedule is controlled to a small value, such as within a three-minute window. Another finding of the study is that system delay, measured as the sum of arrival delays, is smaller when flights are scheduled in the order of arrival compared to in the order of departure. Because flights from airports within the freeze horizon are scheduled in the order of departure, an increase in the number of internal airports with a larger freeze horizon increases system delay. Delay in the given scenario was found to increase by 126% (from 13.8 hours to 31.2 hours) as freeze horizon was increased from 30-minutes to 2-hours in the baseline scenario.

I. INTRODUCTION

Automated tactical scheduling of departure traffic for joining a constrained enroute or arrival traffic flow is one of the steps needed for integrating arrival, departure, surface and enroute operations. Tactical scheduling of departures is accomplished by a Call For Release (CFR) procedure, also known as the Approval Request (APREQ) procedure, which requires the Air Traffic Control Tower (ATCT) to seek permission from the Air Route Traffic Control Center (ARTCC) prior to departure release. Reference 1 describes the Precision Departure Release Capability (PDRC) operational concept and system design for automating the CFR process using the “outbound” and “inbound” scheduling functions of the Traffic Management Advisor (TMA) developed by the National Aeronautics and Space Administration (NASA) and the Federal Aviation Administration (FAA). FAA has since renamed TMA as Time-Based Flow Management (TBFM).

PDRC uses TBFM’s Enroute Departure Capability (EDC) function for outbound scheduling of departure flights from airports included in the CFR within the ARTCC to meter points within the ARTCC. It uses TBFM’s arrival metering called “internal” departure function for scheduling departures into inbound arrival streams of TBFM-metered airports when they are departing from an airport within the arrival freeze horizon. In addition to these functions, a Coupled Scheduling

function for connecting EDC schedules generated in one ARTCC with arrival metering in an adjacent ARTCC has been available in TBFM versions since 2011. This function binds the outbound and inbound tactical departure scheduling.

This report is focused on inbound scheduling. It augments the study in Ref. 2 that examined the benefit of scheduling CFR flights prior to gate pushback compared to upon gate pushback. The earlier study (Ref. 2) assumed gate departure time and taxi-out time uncertainties for 77 major U. S. airports that were characterized based on real-world data. The study scenario consisted of 27 hours of traffic from January 2, 2011 to January 3, 2011 with 37,346 flights from 1,552 airports to 1,357 airports. Arrival capacities at the 77 major U. S. airports were obtained from the FAA's Aviation System Performance Metrics (ASPM) database. Other airports were assumed to be unconstrained so that the traffic bound for these airports would not be delayed by the arrival scheduler. All flights to all airports were assumed to be CFR flights. Delayed departures resulting from gate departure time and taxi-out time uncertainties were allowed to increase speed by up to 2.5% to arrive at the slot reserved at gate pushback or prior to gate pushback. Statistics of ground and airborne delays were obtained by running 100,000 Monte Carlo simulations with a First-Come First-Served (FCFS) arrival scheduler for each of the five look-ahead times- from at pushback (zero look-ahead time) to 60 minutes prior to pushback in 15-minute intervals. The main finding of the study in Ref. 2 is that scheduling should be done at gate pushback because a slot assigned prior to gate pushback is usually lost due to the combination of gate departure time and taxi time uncertainties. The cost of delay (weighted delay), which is measured as the sum of two-times airborne delay and one-time ground delay, increases for longer look-ahead times. Without uncertainty, there is a slight advantage for scheduling early as delay otherwise taken in the air can be transferred to the ground; transfer of delay to the ground decreases the overall weighted delay.

This study examines 808 flights originating from 173 airports destined for Houston George Bush Intercontinental Airport (IAH) within the 27-hour interval from January 2, 2011 to January 3, 2011, the same period considered in Ref. 2. The 808 flights to IAH are a subset of the flights used in the earlier study. The first objective of using this dataset is to see if there is a marked advantage for CFR flights when mixed in with non-CFR ones. The second objective is to determine total system delay in several scenarios with CFR and non-CFR flights. As in the previous study, this study also employs the concept of look-ahead time and introduces the concept of freeze horizon for internal departures. Using an updated FCFS scheduler, three overall categories of simulations were run: 1) all flights are CFR flights, 2) all flights are non-CFR flights and 3) a mix of CFR and non-CFR flights.

Analysis of the results of these scenarios show that CFR flights have an advantage of early scheduling over non-CFR flights when they originate from airports within the freeze horizon, provided the wheels-off time uncertainty of the CFR flights can be controlled to a small value like within a three-minute window, and the freeze horizon is smaller than the sum of the look-ahead time and the flight time to the destination airport. If the gate departure time uncertainty of CFR flights is high, the benefit of early scheduling is lost. Reallocation of new slots for missed slots increases delay, especially airborne delay. It is best to schedule at gate pushback in such situations. System delay results show that scheduling based on estimated time of arrival in the order of arrivals leads to less delay compared to in the order of departures. The implication of ordering by departures is that an arrival slot that could have been given to a later departure that arrives earlier is not available for assignment because an earlier departure had been assigned that slot since it was scheduled earlier. This would result in a delay for the later departure. A longer freeze horizon causes more flights to be scheduled in the order of departure, and therefore it causes the system delay to increase. However, the greatest system delay was observed at the longest look-ahead time in the all CFR flights scenario due to increasing gate departure time uncertainty with increasing look-ahead time.

The rest of the technical memo is organized as follows. Section II describes the IAH arrival scenario and defines freeze horizon, look-ahead time, CFR and non-CFR flights, external and internal airports and the scheduling process. Section III provides descriptions of the gate

departure delay and taxi-out delay distribution modeling using ASPM Data, Airspace Concept Evaluation System (ACES) and the FCFS scheduler. The block diagram in this section outlines the procedure for preparing the input for the scheduler using ACES simulated flight time and for scheduling and re-scheduling CFR flights, and non-CFR internal departures and external departures. Statistics of ground, airborne and weighted delay for the different traffic scenarios are discussed in Section IV. System delay results for these scenarios are also discussed in this section. Finally, the main findings are stated in Section V, the conclusions section.

II. STUDY SCENARIO AND SCHEDULING PROCEDURE

The following section describes the traffic scenario used in this study and the manner in which scheduling is handled for internal, external, CFR and non-CFR flights.

A. Traffic Scenario

The scenario described in this section is tailored for scheduling departures to join an arrival stream at a capacity constrained arrival airport. The concept of freeze horizon from TBFM literature (see Ref. 3) is employed to distinguish between departures from internal and external airports. For simplicity, the freeze horizon in Fig. 1 is represented as a circle centered at the arrival airport where the radius of the circle is the flight time from the periphery of the circle to the arrival airport. All airports inside the circle are referred to as internal airports and airports outside the circle are referred to as external airports. Figure 1 shows the freeze horizon marked by the circle centered at IAH. The two airports – Austin/Bergstrom International Airport (AUS) and Dallas/Fort Worth International Airport (DFW) – are internal airports. The four airports- Hartsfield-Jackson Atlanta International Airport (ATL), Charlotte Douglas International Airport (CLT), Denver International Airport (DEN) and Miami International Airport (MIA) are external airports in this example. The numerical values in the figure indicate average flight time in minutes; for example, the average flight time from DFW to IAH is 44 minutes, whereas it is 135 minutes from MIA to IAH. Freeze horizon for IAH is set between 50 and 250 nautical-miles depending on the arrival meter-fix and the class of aircraft- jets, turboprops and piston-props. For jets it is set between 190 and 250 nautical-miles; this translates to between 46 and 60 minutes assuming an airspeed of 250 knots, which is the maximum allowed airspeed inside the Class-B airspace. The freeze horizon shown in Fig. 1 corresponds to approximately 50 minutes flight time with respect to IAH. In simulations with a mix of CFR and non-CFR flights, only flights from DFW are assumed to be CFR flights. Flights from all other airports including internal airports like AUS are considered to be non-CFR flights.

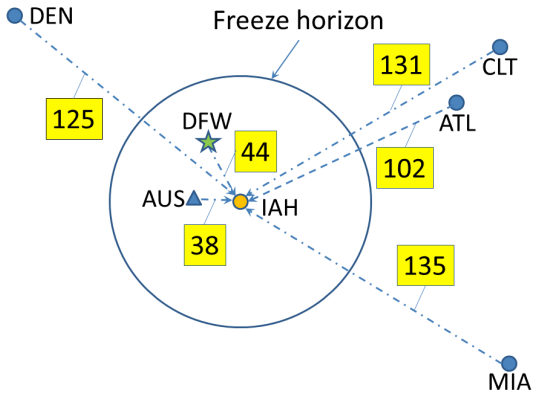

Figure 1. Traffic scenario.

The scenario encompasses departures within 27 hours spanning 9:00 p.m. (3:00 Coordinated Universal Time (UTC)) January 2nd, 2011 through midnight Central Standard Time (CST) (6:00 UTC) January 3rd, 2011 from 173 airports, including the ones in Fig. 1. Out of 808 departures from these airports, 16 are from DFW. ACES, discussed in Section III, was used to simulate 33 hours of air traffic to enable all flights that departed within the 27 hours to land at IAH. Results were generated for different freeze horizon and look-ahead time values using the flight times computed by ACES along with the IAH arrival rate constraint in the FCFS scheduler, which is also described in Section III.

Figure 2 shows the number of internal airports in this study as a function of freeze horizon in minutes. For the maximum value of freeze horizon of 120 minutes, 81 airports are inside the freeze horizon. This means that at least 92 airports (173 minus 81 airports) are outside the freeze horizon. All airports are external airports for a freeze horizon below 40 minutes. Six airports (accounting for 16 departures) are internal airports at the freeze horizon of 40 minutes. At the far end- 120 minutes, 417 flights depart from the 81 internal airports. DFW becomes an internal airport starting at a freeze horizon of 45 minutes. Note that TBFM uses a fixed freeze horizon in real operations. This study does not propose a changing freeze horizon; it uses freeze horizon as a parameter to determine the interaction between look-ahead times and freeze horizon values.

B. Scheduling of CFR and Non-CFR Flights

For CFR flights, which are only from DFW in this scenario, departure scheduling is done in two different ways- at gate pushback (zero look-ahead time) and prior to gate pushback with look-ahead times spanning from 15 minutes to 60 minutes in 15-minute intervals. When scheduling is done at gate pushback, an arrival slot is assigned based on arrival time determined using wheels-off time and flight time estimates, and the assigned delay is taken on the ground. Taxi-out time uncertainty limited to a three-minute window of two-minutes early to one-minute late [-2, +1] (see Ref. 1 Section III.B) with respect to the nominal taxi-out time is permitted; because scheduling is done at gate pushback in this instance, the wheels-off time uncertainty with respect to the scheduled wheels-off time is also bounded by the [-2, +1] minute range of the taxi-out time uncertainty. Limited taxi uncertainty is based on the assumption that CFR flights are given priority on the surface during the taxi-out phase. To account for this uncertainty, once airborne, delayed flights can increase their nominal speed by up to 2.5% and early flights can reduce their nominal speed by up to 5% to get to their assigned arrival slot. This amount of speed adjustment was found to be adequate in this study for CFR flights to not miss their slots. Aircraft are thrust limited at altitude and have a very limited capability for increasing speed. For example, cruise Mach at cruise altitude of 35,000 feet for several Boeing 777 variants is 0.84 and the maximum Mach is 0.89 (see Specifications by model table in Ref. 4). This speed difference translates to a 6% difference with respect to cruise Mach. Large deviation from the optimal cruise speed is also undesirable because it increases fuel consumption.

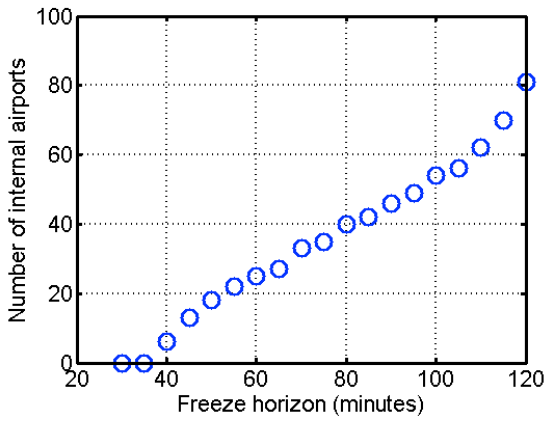

Figure 2. Number of internal airports as a function of freeze horizon.

When scheduling is done for CFR flights prior to gate pushback, an arrival slot corresponding to an arrival time, which is derived from estimated wheels-off time and flight time, is requested at a look-ahead time prior to the proposed gate departure time. This procedure enables earlier slot reservation. Delay assigned by the scheduler is taken on the ground. Next, gate departure time and taxi-time uncertainties are compared with the delay. The larger of the two is added to the proposed gate departure time and nominal taxi-time. The sum is determined to be the actual wheels-off time. Starting with a value of 1.15 for look-ahead time of 15 minutes, the factor for scaling gate departure time uncertainty is increased by 0.05 with increasing look-ahead times in steps of 15-minutes. Thus, the scale factor is 1.2 at 30-minutes and 1.3 at 60-minutes look-ahead times (see Ref. 5). Taxi-out time uncertainty is limited to [-2, +1] minutes. Once airborne, if it is determined that the delayed departures will not be able to make up for the lost time by increasing their speed by 2.5%, the assigned slots are freed up and made available

to other flights; new slots are assigned with additional delays taken in the airborne phase by flying a longer route or by holding in a holding pattern. Two sets of scenarios are discussed later in the results section, 1) with gate departure time uncertainties scaled as a function of look-ahead times according to Ref. 5 and taxi-time uncertainty limited to [-2, + 1] minutes and 2) with controlled wheels-off time uncertainty of [-2, +1] minutes with respect to the scheduled wheels-off time, where the scheduled wheels-off time is obtained as the sum of proposed gate departure time, nominal taxi-time and scheduler assigned delay. Wheels-off time uncertainty is controlled by controlling the combination of the gate departure time and taxi-time uncertainties.

Non-CFR flights from internal airports are scheduled at gate pushback based on wheels-off time and flight time estimates. There is no option for scheduling prior to gate pushback for non-CFR flights. In both types of flights, actual wheels-off time is determined based on delay assigned by the scheduler and taxi-time uncertainty, discussed in Section III. Taxi-time uncertainty is same for CFR and non-CFR flights; it is unique to each airport. Departures are allowed to recover lost or gained time, caused by taxi-time uncertainty, by increasing average speed by up to 2.5% or by decreasing it by up to 5% in the airborne phase. In instances when this adjustment is inadequate to make it to the assigned slot, the slot is freed up and made available to other flights; a new slot is then assigned to the flight with additional delays taken in the airborne phase.

Flights from external airports are non-CFR flights that are airborne by the time they arrive at the freeze horizon. Upon crossing the freeze horizon, an arrival slot is assigned to them by the FCFS scheduler and their scheduled time of arrival at the destination airport is frozen. Any delay assigned by the scheduler is taken in the airborne phase. Being airborne at the time of scheduling means that the scheduling is unaffected by wheels-off time uncertainties, therefore these flights do not miss the assigned slots.

III. DEPARTURE DELAY MODEL AND SOFTWARE SIMULATION TOOLS

Modeling of gate departure delay and taxi-out delay distributions using real-world data derived from the FAA's ASPM database is described in Section III.A. Brief descriptions of ACES and the FCFS scheduler are provided in sections III.B and III.C.

A. Gate Departure Delay and Taxi-out Delay Distribution Modeling

The FAA uses ASPM data, which are accessible on the web for authorized users, for monitoring airport efficiency, aspects of system performance, and retrospective trend analysis studies. The ASPM database provides detailed data on flights to and from the 77 major U. S. airports (ASPM 77 airports) and flights operated by 29 major carriers (ASPM 29 carriers). Flights operated by ASPM carriers between ASPM airports and international and domestic non-ASPM airports are included. Information on airport weather, runway configuration, and arrival and departure rates are also available in the database. ASPM data are useful for gaining insight into air traffic and air carrier activity.

To model gate departure delay and taxi-out delay distributions, hourly average gate departure delays and hourly average taxi-out delays in minutes were derived for each of the 77 major U. S. airports in the ASPM database for each hour of every day in 2011 using the standard "Analysis-By-Airport-By-Hour Report (compared to flight plan)." Gate departure delay is defined as the difference between actual gate-out time and the flight-plan gate-out time. Taxi-out delay is defined as the difference between taxi-out time and unimpeded taxi-out time, where unimpeded taxi-out time is defined as the average time (a single value for each airport) taken to taxi out when congestion, weather, or other delay factors are insignificant. The unimpeded taxi-out times (nominal taxi-out times) for the airports were also obtained from the ASPM database.

Histograms of hourly average gate departure delay and hourly average taxi-out delay in minutes for Hartsfield-Jackson Atlanta International airport are shown in Figs. 3a and 3b. There are 8,727 samples (approximately 24 hours $\times$ 365 days) in the histogram, with data missing for some hours on some days. Observe that data are shown from 0 up to 60 minutes; ASPM database reports non-negative delays. The maximum hourly average gate departure and taxi-out delays were found to be 4.6 hours and 2.4 hours, respectively. Outliers such as these are not shown in the figures. These histograms are modeled with log-delay distributions in this study.

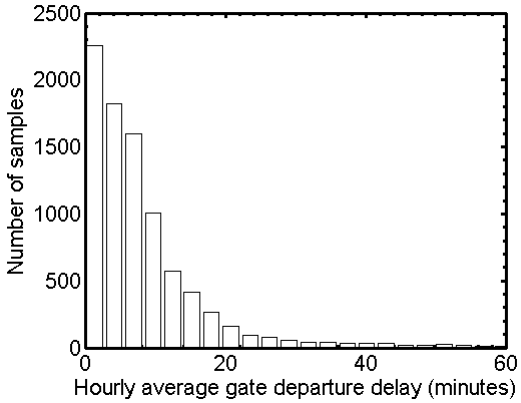

Figure 3a. ATL gate departure delay distribution.

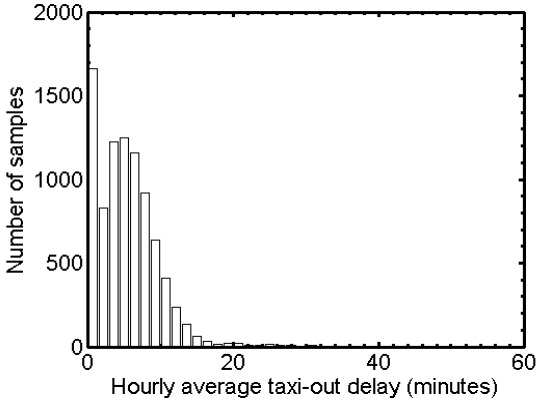

Figure 3b. ATL taxi-out delay distribution.

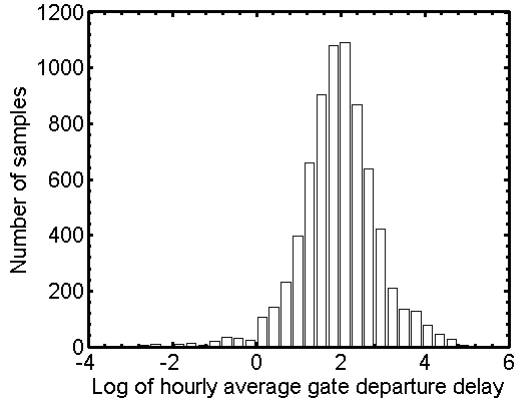

Figure 3c. ATL gate departure log-delay distribution.

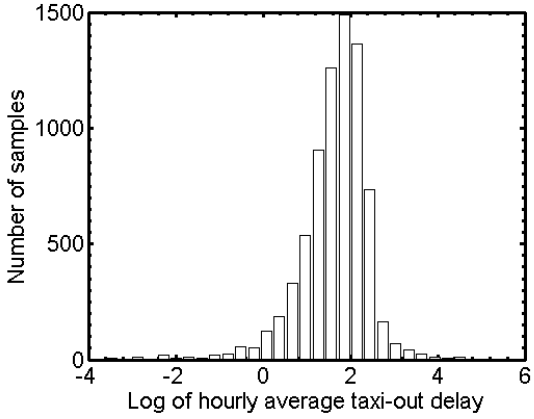

Figure 3d. ATL taxi-out log-delay distribution.

To construct the log-delay distribution, zero delay values were first separated from positive delay values. Natural logarithm of the positive values was then computed and their distribution was determined. Figures 3c and 3d show the resulting histograms of the logarithm of hourly average gate departure and taxi-out delays, where the delays are in minutes. Both of these distributions are modeled by Gaussian distributions with means and standard deviation values computed from the log-delay distributions in spite of the fact that the log-delay distributions fail the Anderson-Darling test for normality. Probability Density Functions (PDF) and Cumulative Distribution Functions (CDF) of the log-delay and the Gaussian distributions are discussed in the context of modeling in the Appendix.

To account for the zero-delay values in the model, a probability of zero-delay is computed as the ratio of the number of zero-delay samples to the total number of samples. For Atlanta,

the zero hourly average gate departure delay and taxi-out delay samples were found to be 1,410 and 1,249, respectively. The probabilities of zero hourly average gate departure and taxi-out delays are thus 0.16 and 0.14 with 8,727 total samples. Data for the 77 airports are given in the Table 3 in the Appendix.

The first step of simulating gate departure and taxi-out delays of a flight from one of the 77 ASPM airports consists of generating a uniformly distributed pseudo-random number between zero and one. If this value is less than or equal to the zero-delay probability value in column two for gate departure delay in Table 3 in the Appendix and in column five for taxi-out delay in the same table, zero delay is assigned. When the value is greater than the zero-delay probability, the second step consists of generating a normally distributed pseudo-random number with mean and standard deviation values specified in Table 3 in the Appendix. If the numerical value of the pseudo-random number is x, delay δ is obtained as

$$\delta = e^{x} \tag{1}$$

These two steps are used to model the distributions shown in Figs. 3a and 3b.

B. Airspace Concept Evaluation System

ACES is a gate-to-gate simulation of air traffic developed at NASA Ames Research Center.[6] ACES simulates flight trajectories using aircraft models derived from the Base of Aircraft Data (BADA) (Ref. 7) and traffic data consisting of departure times and flight-plans obtained from recorded Aircraft Situation Display to Industry (ASDI) files. For each flight in the flight-set to be simulated, ACES takes as input a flight-plan, which includes names of arrival and departure airports, aircraft type (for example, Boeing 737), cruise speed, cruise altitude and route in terms of a series of latitude-longitude pairs. Typical ACES outputs include aircraft state such as position and velocity as a function of time, and system performance metrics such as arrival, departure, en-route and total delays. Validation studies in Refs. 8 and 9 have shown that ACES generates delays and metrics comparable to those observed in the real world. Although ACES can delay flights on the ground and in the air to comply with airport and airspace capacity constraints, this capability was not used in this study. Instead, unconstrained flight times of 808 flights to IAH were determined without capacity constraints. These flight times and proposed wheels-off times are provided to the FCFS scheduler for arrival slot reservation and delay assignment.

C. First-Come First-Served Scheduler

The FCFS scheduler, as the name suggests, schedules arrival slots in the order requested based on airport arrival rate constraints. Input to the scheduler consists of flight times derived from trajectories generated during ACES simulation of unconstrained traffic and proposed wheels-off times obtained by summing the proposed gate departure times from flight-plans and unimpeded taxi-times for airports of departure from ASPM. FCFS also takes as input the taxi and gate uncertainty distributions described in subsection A, and the ASPM-based hourly airport arrival rate constraint. The airport arrival rate constraints are converted into temporal spacing constraints. For example, arrival rate constraints between 68 and 100 flights per hour at IAH for the period of this scenario translated into spacing constraints of 0.88 to 0.6 minutes between successive flights. Note that even when the hourly arrival capacity is greater than hourly demand, delays result due to competition for the same slot by multiple flights given that slots are spaced by at least the minimum spacing constraint described above.

The block-diagram in Fig. 4 summarizes the procedure for scheduling and re-scheduling CFR flights, non-CFR flights, internal airport departures and external airport departures, which were discussed earlier in Section II. Recall that the scheduler estimates the arrival time as the

sum of proposed gate departure time, unimpeded taxi-out time and flight time; it attempts to assign a slot for this arrival time. If unsuccessful, it allocates the next available slot and asks for the flight to be delayed either on the ground or in the air depending on the state of flight at the time of scheduling. If a flight departs late due to uncertainties after taking the assigned delay on the ground, to the extent that the reserved slot cannot be reached after increasing or decreasing its speed, the reserved slot is reclaimed by the scheduler and a new slot and airborne delay are assigned. Flights from external airports are assigned an arrival slot when they cross the freeze horizon and the scheduling delay is taken in the air inside the freeze horizon. A new slot is always spaced with respect to previously assigned slots based on the airport arrival rate constraint, which typically varies throughout the day. From a practical standpoint, this means that an early slot reservation request for a slot at a later time requires an airport arrival rate constraint forecast at that later time. Poor arrival rate constraint forecasting can lead to the assignment of a slot that does not materialize at the target time or a slot that is not assigned but appears at the target time in the future. In this study, perfect knowledge of arrival rate constraint is assumed.

The following example illustrates the scheduling procedure for a CFR flight from DFW in which an arrival slot at IAH is requested at 9:00 a.m. for an expected 10:00 a.m. gate departure time. Given that DFW unimpeded taxi-out time is 11 minutes and flight time from DFW to IAH is 44 minutes, the scheduler attempts to reserve a 10:55 a.m. slot (arrival time estimate = expected gate departure at 10:00 a.m. + unimpeded taxi time of 11 minutes + nominal flight time

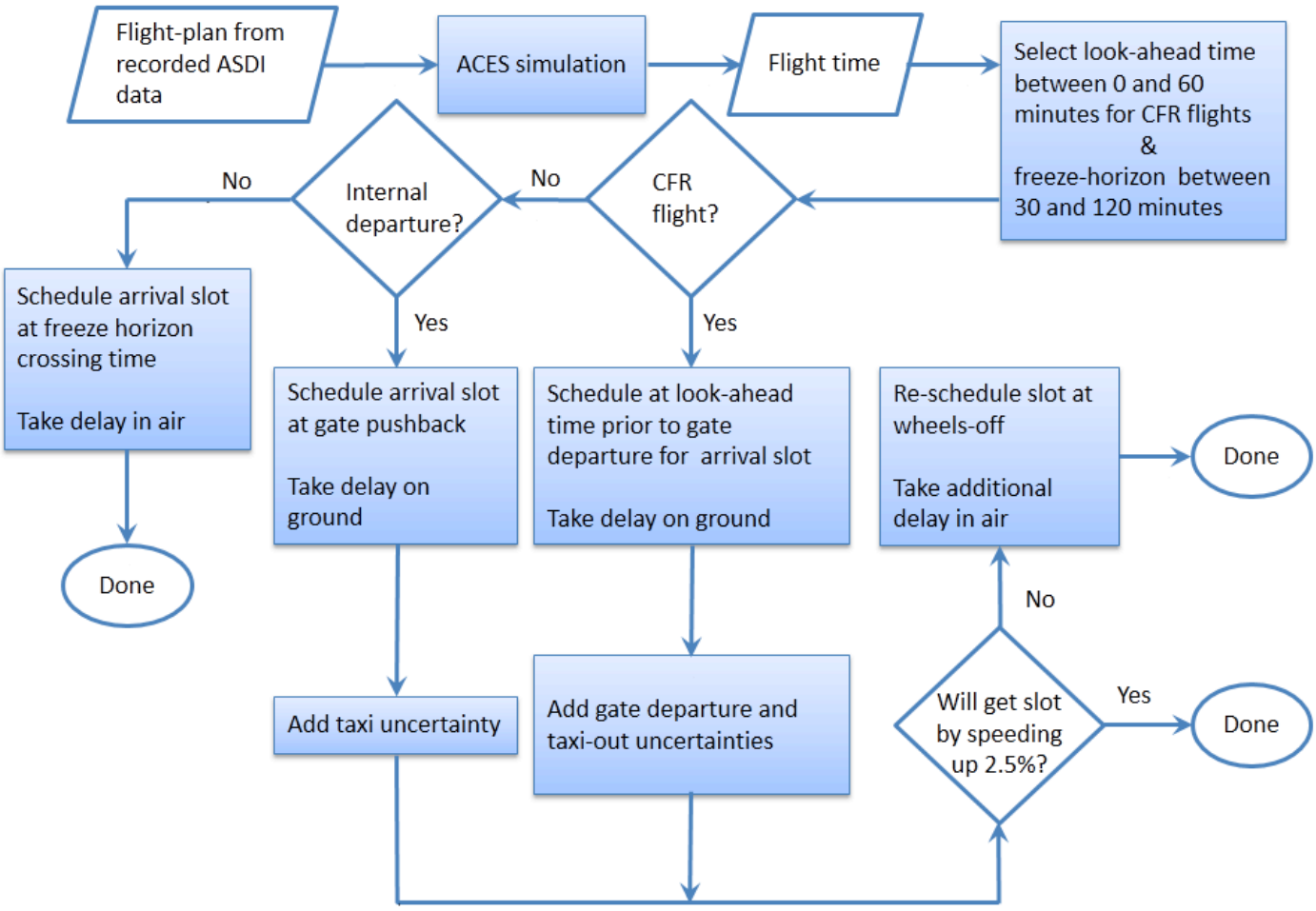

Figure 4. FCFS scheduling process.

of 44 minutes). In this example, the 10:55 a.m. slot is already occupied therefore the next available slot at 10:56 a.m. and one-minute of delay are assigned by the scheduler. As a result of gate and taxi-out time uncertainty, the flight actually departs with a wheels-off time of 10:20 a.m. Upon detecting wheels-off, the scheduler estimates the earliest arrival time for this flight to be 11:00 a.m. assuming a 2.5% average speed increase; therefore, it frees up the 10:56 a.m. slot at 10:20 a.m. for other potential arrivals and attempts to assign the 11:00 a.m. slot. Because the 11:00 a.m. slot is also unavailable, the next available slot at 11:01 a.m. is assigned. The flight then takes an additional minute of delay in the airborne phase to arrive at IAH at 11:01 a.m.

IV. RESULTS

Results based on the procedures and tools described in sections II and III are presented in the following subsections. Subsection A describes the scenarios that were run and the reasoning behind them. Subsection B describes the two scenarios in which all flights are CFR flights as in the previous delay sensitivity study in Ref. 2. Subsection C describes the two additional scenarios in which both CFR and non-CFR flights are included. Lastly, Subsection D investigates total system delay in each scenario. These results attempt to answer the question of whether scheduling in advance is beneficial. All flights are IAH bound in these scenarios. In scenarios with CFR and non-CFR flights, only flights departing from DFW are considered to be CFR flights. Results are based on Monte-Carlo simulations in which each scenario is run 10,000 times with randomized taxi time and gate departure time uncertainties.

A. Description of Scenarios

Three scenarios and their variations are presented in Table 1. The scenarios are characterized by (a) the extent of CFR flights- (1) none of the flights are CFR flights, (2) all flights are CFR flights and (3) only flights departing DFW are CFR flights, and by (b) wheels-off time prediction uncertainty- (1) wheels-off time uncertainty controlled to [-2, +1] minutes and (2) wheels-off time uncertainty is not controlled (sampled from distributions such as in Figures 3c and 3d as described in Section III). For the remainder of Section IV, scenarios will be referred by their scenario number listed in Table 1.

Table 1. Scenario summary

Scenario #	Description	Motivation
0	None of the flights are CFR flights.	Baseline scenario.
1a	All flights are CFR flights and wheels-off time uncertainty is not controlled.	For comparison with conclusions of the earlier study in Ref. 2.
1b	All flights are CFR flights and wheels-off time uncertainty is controlled.	Same reason as 1a.
2a	Only DFW flights are CFR flights and wheels-off time uncertainty is not controlled.	Focal point of this study- to investigate the benefits to CFR flights over non-CFR flights.
2b	Only DFW flights are CFR flights and wheels-off time uncertainty is controlled.	Same reason as 2a.

B. All Flights are CFR Flights

This section describes the results of scenarios 1a and 1b in terms of delay per flight. These scenarios were run for comparison with the findings of the earlier delay sensitivity study, Ref. 2, in which all flights were CFR flights.

Figure 5a presents the average weighted delay per flight in minutes, where the average is taken over 10,000 Monte Carlo runs and 808 departures, as a function of scheduling from 0 to 60 minutes prior to the proposed gate departure time. Because gate departure time uncertainty is larger for longer look-ahead times (see Ref. 5), more flights fail to depart at the gate departure time assumed during slot assignment; this causes them to miss their scheduled arrival slot. These slots often cannot be assigned to later flights. Rescheduling to assign new arrival slots for missed slots also reduces the number of available slots at later times, which causes the overall system delay to increase. Thus, as look-ahead time increases, delay increases as depicted in Fig. 5a. This trend is consistent with the findings in the previous delay sensitivity study summarized in Ref. 2.

Results for the second scenario- 1b are summarized in Figure 5b. Wheels-off time uncertainty is limited to [-2, +1] minutes in this scenario. Comparing Figs. 5b to 5a it is seen that limiting wheels-off time uncertainty causes the delay to remain constant with increasing look-ahead times and the amount of delay is the same as zero-minutes CFR look-ahead under uncontrolled uncertainty, which implies that there is no advantage to scheduling in advance of

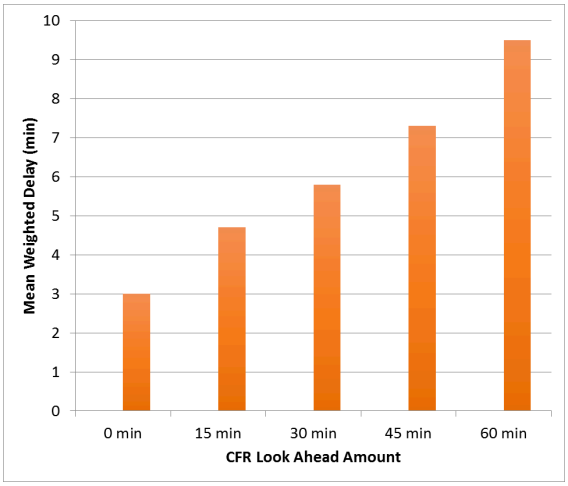

Figure 5a. Average weighted delay per flight when uncertainty is not controlled and all flights are CFR flights.

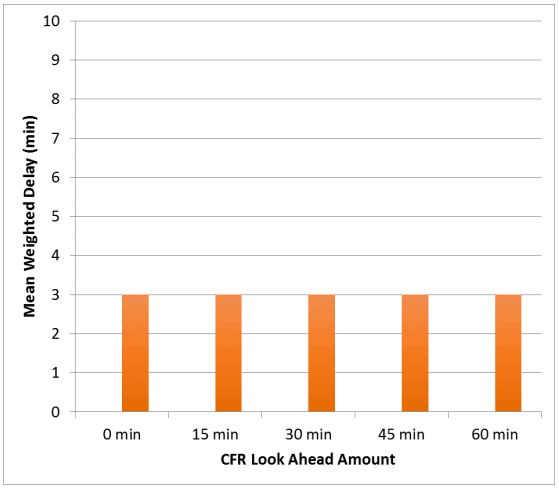

Figure 5b. Average weighted delay per flight when uncertainty is controlled and all flights are CFR flights.

gate departure. The main reason is that scheduling all flights equally early with small wheels-off time uncertainty does not change the arrival sequence and congestion at the arrival airport. Earlier in Ref. 2 it was determined that without gate departure time and taxi-out time uncertainties, scheduling in advance offered a slight advantage. Total delay could be lowered by re-sequencing flights and more of the scheduling delay could be passed to the ground with longer look-ahead times. Results in Fig. 5b do not show such an advantage because they are based on strict FCFS without re-sequencing.

Although results in Figs. 5a and 5b showed no advantage to scheduling in advance of gate pushback, even when uncertainty is small, it is important to note that only the capacity of the arrival airport was taken into account by the scheduler. If other constraints such as the capacity of the departure airport were taken into account, it is possible that the time gained by scheduling in advance of gate departure could be used for improving coordination with downstream facilities and scheduling of surface traffic, which could lower system-wide delays.

C. Mix of CFR and Non-CFR Flights

Results of 2a and 2b scenarios are discussed in this section. Only flights from DFW are CFR flights in both these scenarios. As in Scenario 1a, gate departure time uncertainty increases for CFR flights with longer look-ahead times in Scenario 2a. Taxi time uncertainty is limited to -2 to +1 minutes with respect to the unimpeded taxi-out time. Wheels-off time uncertainty for CFR flights is restricted to -2 to +1 minutes in Scenario 2b like in Scenario 1b. CFR flights are scheduled from 0 to 60 minutes prior to their proposed gate pushback time. Non-CFR flights outside the freeze horizon, which is set in a range of 30 to 120 minutes of flight time to IAH, are scheduled when they cross the freeze horizon. These flights are not affected by gate departure time and taxi-out time uncertainty because they are already airborne by the time they cross the freeze horizon. Non-CFR flights within the freeze horizon are scheduled at their gate departure time; taxi-out time for these flights in Scenario 2a is obtained by sampling the taxi-out delay distribution and in Scenario 2b is limited to within -2 to +1 minutes.

Results of 10,000 Monte Carlo runs for Scenario 2a are summarized in Figs. 6a and 6b. Figure 6a and 6b show the average weighted delay per CFR flight and per non-CFR flight, respectively, as a function of freeze horizon and look-ahead time. Averages were determined based on 16 CFR flights from DFW and 792 non-CFR flights from the other 172 airports. Figure 6a shows that there is no advantage to scheduling in advance. The graph corresponding to scheduling at gate departure time is always below the graphs corresponding to scheduling at longer look-ahead times. Furthermore, observe the bi-modal behavior with one being the graphs corresponding to longer look-ahead times bunched together and the other being the graph corresponding to at gate departure time. Whereas the standard deviation of gate departure delay distribution increases by 30% from look-ahead time of zero to 60 minutes, delay does not change significantly in the 15-minute to 60-minute look-ahead time range; it remains primarily a function of freeze horizon. Figure 6b shows that the delays of non-CFR flights are very similar in magnitude to the delays of CFR flights obtained by scheduling at gate departure time (see zero look-ahead time result in Fig. 6a). This is expected because non-CFR flights inside the freeze horizon are also scheduled at gate departure time. Please note the different y-axis scales of Figs. 6a and 6b; the smaller y-axis scale in Fig. 6b is used to amplify the differences in look-ahead time graphs. Comparing Figs. 6a and 6b it is seen that CFR flights have a lower delay up

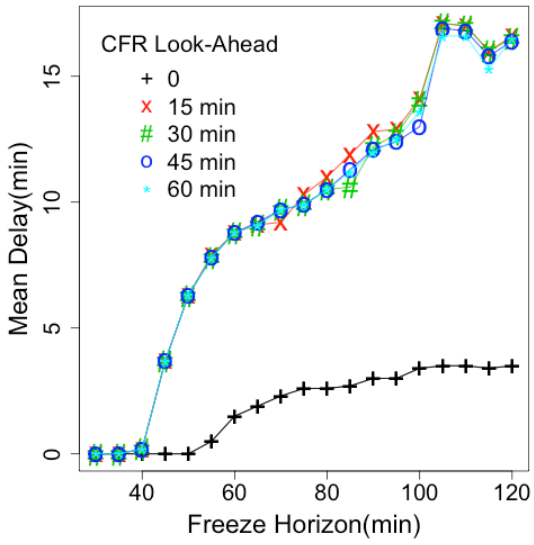

Figure 6a. Average weighted delay per CFR flight from DFW when uncertainty is uncontrolled.

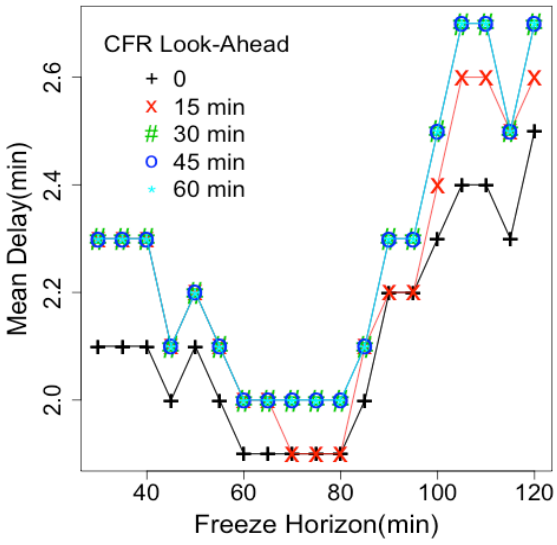

Figure 6b. Average weighted delay per non-CFR flight when uncertainty is uncontrolled.

to the freeze horizon value of about 45 minutes. The reason is that CFR flights get scheduled prior to both external and internal non-CFR flights for freeze horizon values smaller than the average flight time from DFW to IAH, which is 44 minutes. For example, a CFR flight would be scheduled at 9:16 a.m. at the latest for an arrival slot at 10:00 a.m. With a freeze horizon of 40 minutes or less, a non-CFR flight also competing for the same arrival slot at 10:00 a.m. will be scheduled at 9:20 a.m. at the earliest, after the CFR flight has already been scheduled. Delay increase for non-CFR flights at longer freeze horizon values seen in Fig. 6b is due to more airports, therefore more flights, being included inside the freeze horizon; flights from these airports are affected by taxi-out time uncertainty compared to those outside the freeze horizon that do not have uncertainty at the time of scheduling.

Figures 7a and 7b show the Scenario 2b average weighted delay results for CFR and non-CFR flights, respectively. Figure 7a shows that up to a freeze horizon of 50 minutes, there is no advantage to scheduling early. As the freeze horizon is increased, more non-CFR flights get an advantage by scheduling earlier compared to CFR flights from DFW, which are about 44 minutes away from IAH. Observe the increasing delay as a function of freeze horizon in Fig. 7a when CFR flights are scheduled at gate departure time compared to an initial decrease in delay of non-CFR flights in Fig. 7b. The graphs in Fig. 7a show the delay of CFR flights to be decreasing with longer look-ahead time. Since the wheels-off time uncertainty is kept small and independent of look-ahead time, longer look-ahead time can be thought of as a longer freeze horizon only for CFR flights. This enables CFR flights to schedule earlier than most non-CFR flights. Comparing Fig. 7a to 6a, it is seen that the delay of CFR flights is considerably lower when wheels-off time uncertainty is small. Smaller taxi-out uncertainty has very little impact on average delay of non-CFR flights; this can be observed by comparing Fig. 7b to 6b.

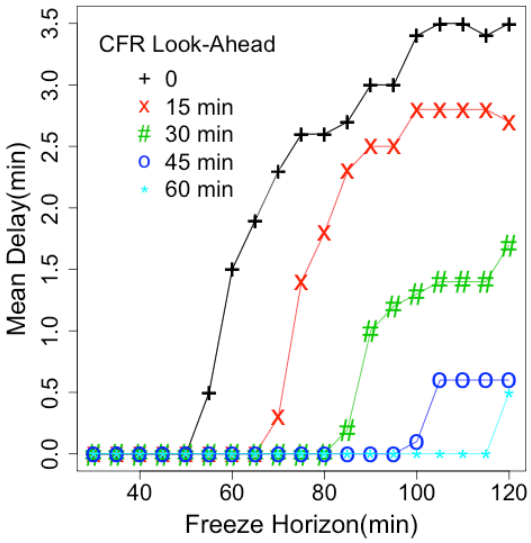

Figure 7a. Average weighted delay per CFR flight when uncertainty is controlled.

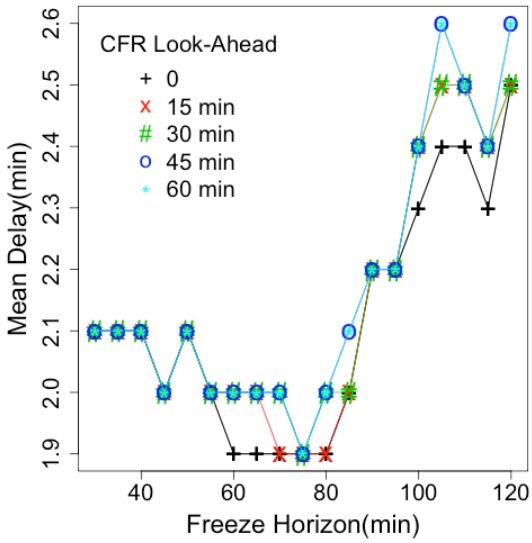

Figure 7b. Average weighted delay per non-CFR flight when uncertainty is controlled.

In summary, CFR flights get an advantage over non-CFR flights if they are scheduled earlier, which happens if the sum of their flight time to destination airport and look-ahead time is larger than the freeze horizon, and the wheels-off time uncertainty is small. If the gate departure time uncertainty is high, it is best to schedule at gate departure time. The freeze horizon distances of 190 to 250 nautical-miles for jets in IAH TBFM translates to freeze horizon times of 38 to 50 minutes assuming an average speed of 300 knots. Results in Figs. 6a and 7a suggest that CFR flights from DFW to IAH should be scheduled at gate departure time for this range of

freeze horizon times; there is no advantage to scheduling earlier even with controlled uncertainty.

D. Total System Delay

Delays for CFR and non-CFR flights were examined in subsections B and C for the five scenarios listed in Table 1; in this section, average system delay measured as the sum of arrival delays (includes both ground and airborne delays) of all flights to IAH is examined. Combinations of look-ahead times and freeze horizons were examined to determine maximum and minimum average total delays. The averages are again based on 10,000 Monte Carlo runs. Results are summarized in Table 2 and in Fig. 8. Minimum and maximum average total delays were found to be 13.8 hours for a freeze horizon of 30 minutes and 31.2 hours for a freeze horizon of 120 minutes, respectively, for the baseline scenario without CFR flights (Scenario 0 in Table 1). Average total delays for the baseline scenario for the range of freeze horizon values are shown in Fig. 9a in the Appendix. The least amount of delay is achieved in this scenario, compared to the delays in other scenarios listed in Table 2, because all flights are scheduled in the order of their arrival. One of the findings in the previous study in Ref. 2 is that system delay increases as arrival slots for more flights are scheduled out of the nominal arrival order.

Table 2. Total system delay summary

Scenario #	Delay (Hrs.)	Look-ahead time and freeze horizon parameters
0 (min)	13.8	Look-ahead time: all, Freeze horizon: 30
0 (max)	31.2	Look-ahead time: all, Freeze horizon: 120
1a (min)	40.2	Look-ahead time: 0, Freeze horizon: all
1a (max)	90.0	Look-ahead time: 60, Freeze horizon: all
1b	40.2	Look-ahead time: all, Freeze horizon: all
2a (min)	14.2	Look-ahead time: 0, Freeze horizon: 30
2a (max)	34.0	Look-ahead time: 60, Freeze horizon: 120
2b (min)	14.2	Look-ahead time: 0, Freeze horizon: 30
2b (max)	30.4	Look-ahead time: 60, Freeze horizon: 120

Because there are no internal airports within the 30-minute freeze horizon, arrival slots are scheduled in the order they would have naturally arrived at IAH. Additionally, because all flights are airborne by the time they are scheduled at the freeze horizon, their scheduled arrival slots are unaffected by gate departure and taxi-out delays, which cause flights to be rescheduled in the other scenarios.

The maximum average system delay occurs in Scenario 1a with a look-ahead time of 60 minutes when all flights are CFR flights and gate departure time uncertainty is not controlled. Results are independent of freeze horizon as seen in Fig. 10a. This is to be expected because there is no distinction between flights inside and outside the freeze horizon; they all are CFR flights. There are two reasons for high delay in this scenario: (1) gate departure delay uncertainty growth with longer look-ahead time causes flights to miss their

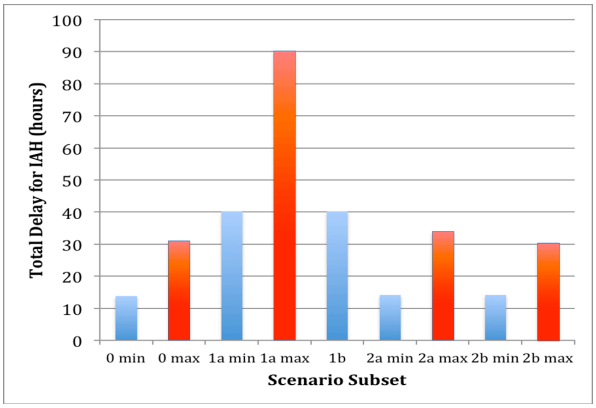

Figure 8. Minimum and maximum values of average total delay.

scheduled slots and (2) all flights are scheduled in the order of departure, i.e. when they leave the gate. When flights miss their arrival slot, they have to be rescheduled and additional delay has to be taken while airborne. Scheduling in the order of departure leads to higher delay compared to scheduling in the order of arrival.

The next set of results for Scenarios 2a and 2b in Table 2 are similar to the results for Scenario 0 as expected; Scenario 2 has only 16 fewer non-CFR flights (16 CFR flights from DFW and 792 non-CFR flights from other airports) compared to Scenario 0 with 808 non-CFR flights. Graphs in Fig. 12a in the Appendix show the average delay to be mostly a function of freeze horizon. Delay increases a bit when scheduling is done prior to gate departure. Graphs for Scenario 2b in Fig. 13a in the Appendix show the average delay to be almost independent of look-ahead time. This is expected because wheels-off time uncertainty is limited.

In summary, the minimum values for scenarios 0, 2a, and 2b in Table 2 show that scheduling in the order of arrival, which is accomplished by setting the freeze horizon to 30 minutes, leads to small average system delay. Maximum values for the same scenarios in Table 2 show that longer freeze horizon leads to large average system delay. Most system delay occurs when all flights are CFR flights and departure time uncertainty is not controlled.

V. CONCLUSIONS

An earlier delay sensitivity concluded scheduling should be done at gate pushback because of gate departure time and taxi time uncertainties. It also concluded that there is a slight advantage of scheduling a flight early for an arrival slot in that the delay needed for temporal spacing can be taken on the ground as opposed to in the air, provided the wheels-off time uncertainty can be controlled to a small value (like -2 minutes early to +1 minute late). All flights were Call For Release flights in the earlier study.

The current study is based on the same simulated air traffic data as the earlier one. Five different scenarios with 808 Call For Release and non-Call For Release flights from 173 airports to Houston George Bush Intercontinental Airport (IAH) were examined. These scenarios either assumed gate departure time uncertainty that increased with look-ahead time or wheels-off time uncertainty that could be limited to -2 minutes early to +1 minute late with respect to the scheduled wheels-off time. Average weighted delays (sum of one-time ground delay + two-times airborne delay) and average arrival delays were computed for these scenarios based on 10,000 Monte Carlo runs using the First-Come First-Served method for scheduling arrivals.

Results show that increasing gate departure time uncertainty as a function of look-ahead time causes the weighted delay to increase as a function of look-ahead time when all flights in the scenario are Call For Release flights. It is detrimental to schedule early in this scenario. It also follows that there is no advantage to early scheduling even if wheels-off time uncertainty is small in this scenario because every Call For Release flight can schedule equally early. These findings are in agreement with the earlier study.

Analysis of scenarios with 16 Call For Release flights from Dallas-Fort Worth Airport (DFW) and 792 non-Call For Release flights from 172 other airports showed that Call For Release flights do get an advantage over the non-Call For Release flights from airports inside the freeze horizon if the sum of the flight time to the destination airport and look-ahead time is longer than the freeze horizon and the wheels-off time uncertainty is small. If gate departure time uncertainty is large, Call For Release flights should be scheduled at gate pushback.

Results in this report show that Call For Release flights from Dallas-Fort Worth to Houston George Bush Intercontinental do not benefit by scheduling prior to gate departure time for a typical Traffic Management Advisor freeze horizon setting of 38 to 50 minutes or an equivalent distance of 190 to 250 nautical-miles. From a system delay (sum of arrival delays of all flights) perspective, the order of scheduling was found to be important. Results show that scheduling in the order of arrival leads to less delay compared to scheduling in the order of departure. Increasing the freeze horizon leads more flights to be scheduled in the order of departure, which

increases system delay. The largest amount of system delay was accrued at the longest look-ahead time in the scenario with all Call For Release flights primarily due to increasing gate departure time uncertainty with longer look-ahead time.

APPENDIX

Table 3 shows the parameters for modeling gate departure and taxi-out time delay distributions shown in Figs. 3a and 3b for the 77 ASPM airports following the procedure described in Section III.A.

Table 3. Hourly average gate departure and taxi-out delay model data

Airport Code	Hourly Average Gate Departure Delay			Hourly Average Taxi-out Delay		
	Zero-Delay Probability	Mean Log-Delay	Standard Deviation Log-Delay	Zero-Delay Probability	Mean Log-Delay	Standard Deviation Log-Delay
ABQ	0.340	1.430	1.230	0.289	0.539	0.945
ANC	0.131	1.434	1.085	0.154	-0.126	1.527
ATL	0.162	1.959	0.918	0.143	1.634	0.803
AUS	0.299	1.677	1.181	0.250	0.174	1.102
BDL	0.313	1.734	1.214	0.272	0.354	1.267
BHM	0.417	1.843	1.306	0.411	0.428	1.089
BNA	0.290	1.689	1.137	0.259	0.469	0.966
BOS	0.198	1.885	0.968	0.179	1.216	0.842
BUF	0.307	1.936	1.257	0.335	0.259	1.280
BUR	0.360	1.530	1.289	0.230	0.333	0.934
BWI	0.215	1.856	1.080	0.202	0.747	0.870
CLE	0.239	1.739	1.107	0.243	0.603	1.099
CLT	0.176	1.920	0.906	0.145	1.425	0.772
CVG	0.297	1.854	1.129	0.313	0.135	1.264
DAL	0.229	1.991	1.032	0.227	0.038	1.036
DAY	0.475	1.739	1.328	0.461	0.522	1.222
DCA	0.224	1.668	1.020	0.191	1.064	0.907
DEN	0.174	1.915	0.983	0.135	0.817	0.928
DFW	0.179	2.026	0.797	0.176	0.918	0.666
DTW	0.224	1.965	0.938	0.227	0.592	1.114
EWR	0.153	2.167	0.977	0.123	1.637	0.901
FLL	0.228	1.803	1.010	0.199	0.962	0.914
GYY	0.938	3.042	1.005	0.986	-0.410	0.186
HNL	0.113	1.077	1.057	0.095	0.276	0.843
HOU	0.258	1.938	1.060	0.253	0.146	0.939
HPN	0.307	2.614	0.966	0.362	0.262	1.300
IAD	0.189	2.229	0.936	0.191	0.646	1.083
IAH	0.206	1.884	0.824	0.180	1.130	0.847
IND	0.204	1.846	1.163	0.249	0.057	1.216
ISP	0.617	1.820	1.419	0.466	-0.006	1.148
JAX	0.340	1.537	1.309	0.257	0.391	1.037

Table 3. Hourly average gate departure and taxi-out delay model data (contd.)

Airport Code	Hourly Average Gate Departure Delay			Hourly Average Taxi-out Delay		
	Zero-Delay Probability	Mean Log-Delay	Standard Deviation Log-Delay	Zero-Delay Probability	Mean Log-Delay	Standard Deviation Log-Delay
JFK	0.110	2.134	0.945	0.093	1.348	1.183
LAS	0.157	1.764	0.855	0.130	1.008	0.706
LAX	0.074	1.842	0.737	0.058	1.102	0.606
LGA	0.203	1.957	1.020	0.181	1.963	0.982
LGB	0.498	1.668	1.301	0.339	0.488	1.129
MCI	0.254	1.656	1.119	0.250	0.327	1.048
MCO	0.222	1.673	1.050	0.168	1.004	0.732
MDW	0.232	2.082	0.952	0.224	0.679	0.883
MEM	0.279	2.148	1.109	0.269	0.326	1.276
MHT	0.383	2.026	1.327	0.407	0.038	1.286
MIA	0.160	2.329	0.802	0.153	0.909	0.699
MKE	0.229	1.880	1.162	0.228	0.360	1.123
MSP	0.266	1.780	0.973	0.237	0.788	0.988
MSY	0.324	1.467	1.282	0.288	0.332	0.982
OAK	0.141	1.778	1.077	0.130	0.005	1.061
OGG	0.539	1.042	1.177	0.316	0.035	0.964
OMA	0.352	1.710	1.205	0.342	0.216	1.207
ONT	0.288	1.756	1.436	0.203	0.083	1.184
ORD	0.109	2.061	0.923	0.098	1.277	0.797
OXR	0.957	3.004	1.060	0.945	1.200	0.459
PBI	0.343	2.190	1.148	0.269	0.372	1.000
PDX	0.210	1.418	1.114	0.172	0.464	0.863
PHL	0.166	2.039	1.005	0.153	1.223	1.147
PHX	0.158	1.617	0.899	0.135	0.877	0.826
PIT	0.242	1.885	1.142	0.281	0.389	1.215
PSP	0.544	2.039	1.240	0.360	0.669	1.074
PVD	0.349	1.877	1.263	0.392	0.442	1.206
RDU	0.253	1.913	1.124	0.243	0.774	0.926
RFD	0.783	2.394	1.381	0.953	-0.482	0.595
RSW	0.373	1.515	1.288	0.275	0.357	1.074
SAN	0.193	1.512	1.107	0.164	0.752	0.792
SAT	0.290	1.597	1.167	0.224	0.579	0.909
SDF	0.250	1.958	1.246	0.323	-0.020	1.302
SEA	0.195	1.285	0.972	0.163	0.595	0.802
SFO	0.137	1.855	0.924	0.120	1.181	0.664
SJC	0.208	1.452	1.200	0.151	0.223	0.915
SJU	0.360	1.610	1.231	0.292	0.234	1.043

Table 3. Hourly average gate departure and taxi-out delay model data (contd.)

Airport Code	Hourly Average Gate Departure Delay			Hourly Average Taxi-out Delay		
	Zero-Delay Probability	Mean Log-Delay	Standard Deviation Log-Delay	Zero-Delay Probability	Mean Log-Delay	Standard Deviation Log-Delay
SLC	0.233	1.492	1.047	0.212	1.038	0.954
SMF	0.203	1.384	1.194	0.146	0.351	0.926
SNA	0.174	1.484	1.144	0.135	0.436	1.142
STL	0.220	1.808	1.036	0.239	0.187	0.955
SWF	0.710	2.641	1.285	0.815	0.171	1.600
TEB	0.269	3.299	0.800	0.853	-0.521	0.333
TPA	0.288	1.414	1.329	0.264	0.450	0.874
TUS	0.476	1.373	1.317	0.271	0.563	1.044
VNY	0.676	3.271	0.905	0.933	-0.426	0.296

Figures 9 through 13 present ground, airborne and weighted delay results for CFR and non-CFR flights, and system delay results for the five scenarios discussed in Table 1. Each figure is composed of sub-figures ‘a’ through ‘m’. The contents of the sub-figures are listed in Table 4. Color coded graphs in the sub-figures are for look-ahead times from at pushback (zero minutes) to 60 minutes prior to expected gate pushback time. The average delay values are shown as a function of freeze horizon in the graphs. Figure 9 shows the results for the baseline scenario without CFR flights (Scenario 0 in Table 1). Results for Scenario 1a and 1b (see Table 1) with all CFR flights are given in Figs. 10 and 11. Mixed scenarios- 2a and 2b results with CFR flights from DFW are provided in Figs. 12 and 13.

Table 4. Contents of sub-figures

Sub-figure	Content
a	Average system delay (total arrival delay at IAH)
b	Average weighted delay per CFR flight
c	Average ground delay per CFR flight
d	Average air delay per CFR flight
e	Average weighted delay per non-CFR flight
f	Average ground delay per non-CFR flight
g	Average air delay per non-CFR flight
h	Average weighted delay per non-CFR external flight
i	Average ground delay per non-CFR external flight
j	Average air delay per non-CFR external flight
k	Average weighted delay per non-CFR internal flight
l	Average ground delay per non-CFR internal flight
m	Average air delay per non-CFR internal flight

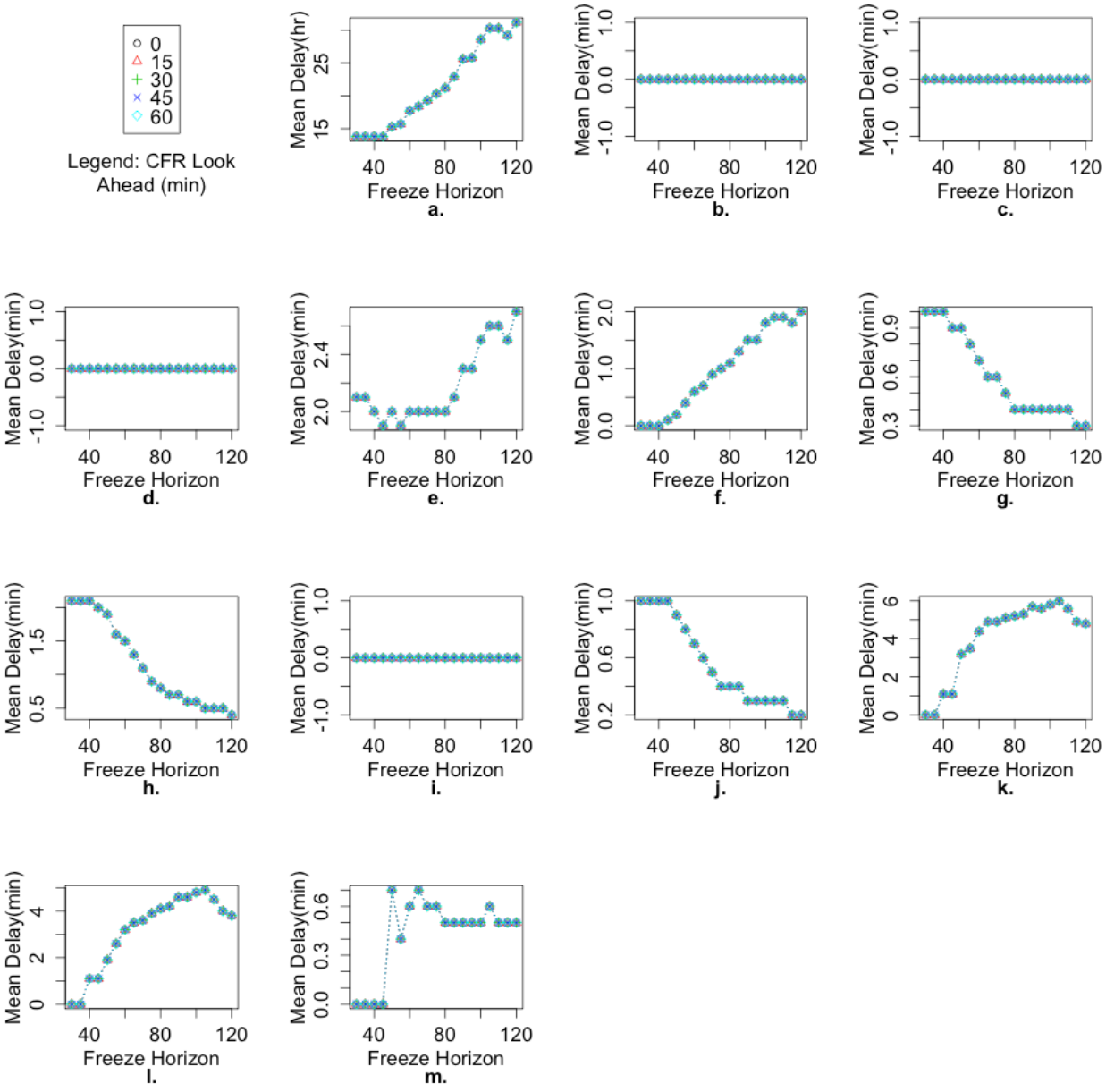

Figure 9. Baseline scenario without CFR flights (Scenario 0 in Table 1).

a. system delay
b. weighted delay/CFR
c. ground delay/CFR
d. air delay/CFR
e. weighted delay/non-CFR
f. ground delay/non-CFR
g. air delay/non-CFR
h. weighted delay/non-CFR external
i. ground delay/non-CFR external
j. air delay/non-CFR external
k. weighted delay/non-CFR internal
l. ground delay/non-CFR internal
m. air delay/non-CFR internal

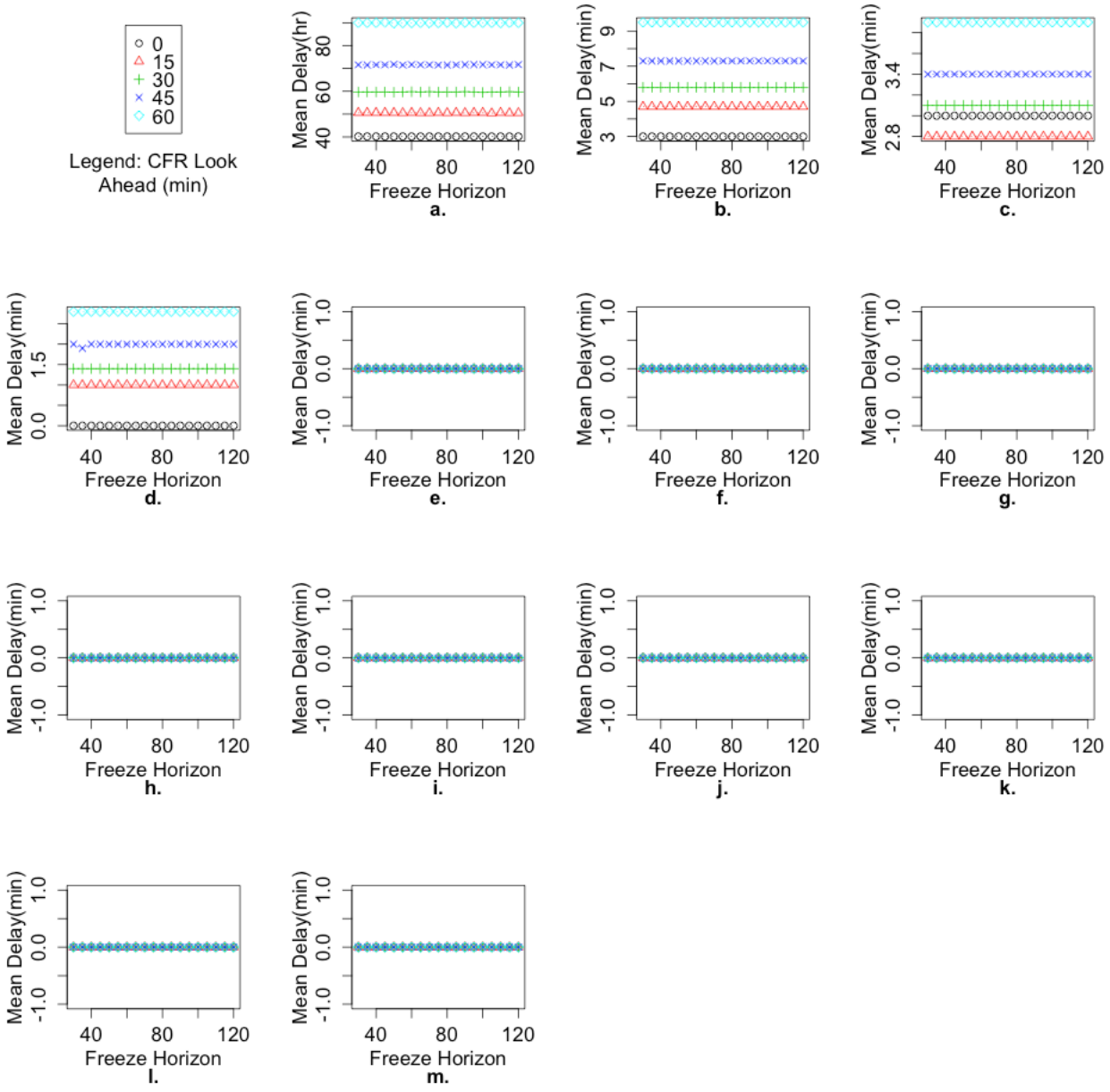

Figure 10. Results for Scenario 1a in which all flights are CFR flights and wheels-off time uncertainty is not controlled.

a. system delay
b. weighted delay/CFR
c. ground delay/CFR
d. air delay/CFR
e. weighted delay/non-CFR
f. ground delay/non-CFR
g. air delay/non-CFR
h. weighted delay/non-CFR external
i. ground delay/non-CFR external
j. air delay/non-CFR external
k. weighted delay/non-CFR internal
l. ground delay/non-CFR internal
m. air delay/non-CFR internal

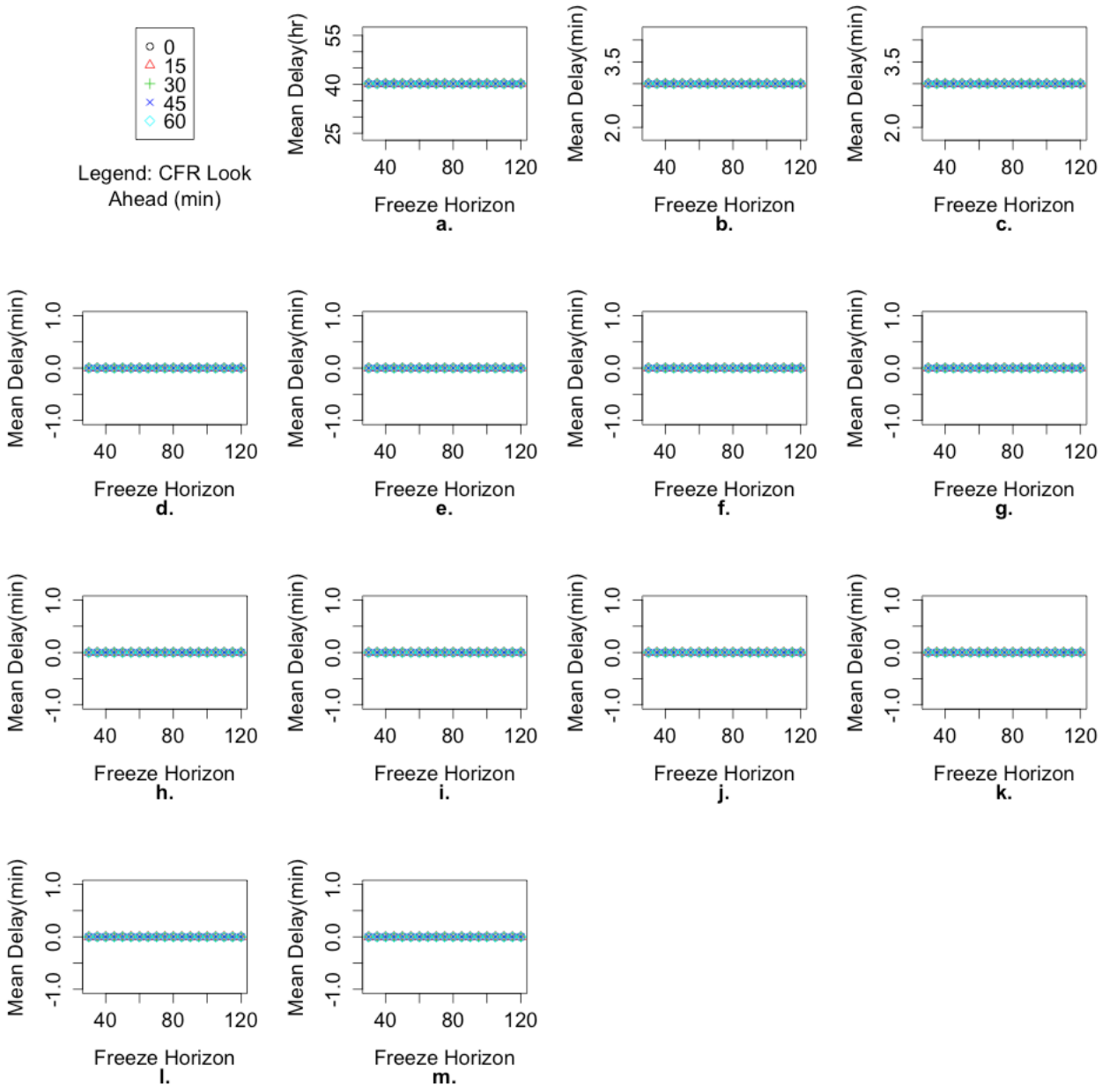

Figure 11. Results for Scenario 1b in which all flights are CFR flights and wheels-off time uncertainty is controlled.

a. system delay
b. weighted delay/CFR
c. ground delay/CFR
d. air delay/CFR
e. weighted delay/non-CFR
f. ground delay/non-CFR
g. air delay/non-CFR
h. weighted delay/non-CFR external
i. ground delay/non-CFR external
j. air delay/non-CFR external
k. weighted delay/non-CFR internal
l. ground delay/non-CFR internal
m. air delay/non-CFR internal

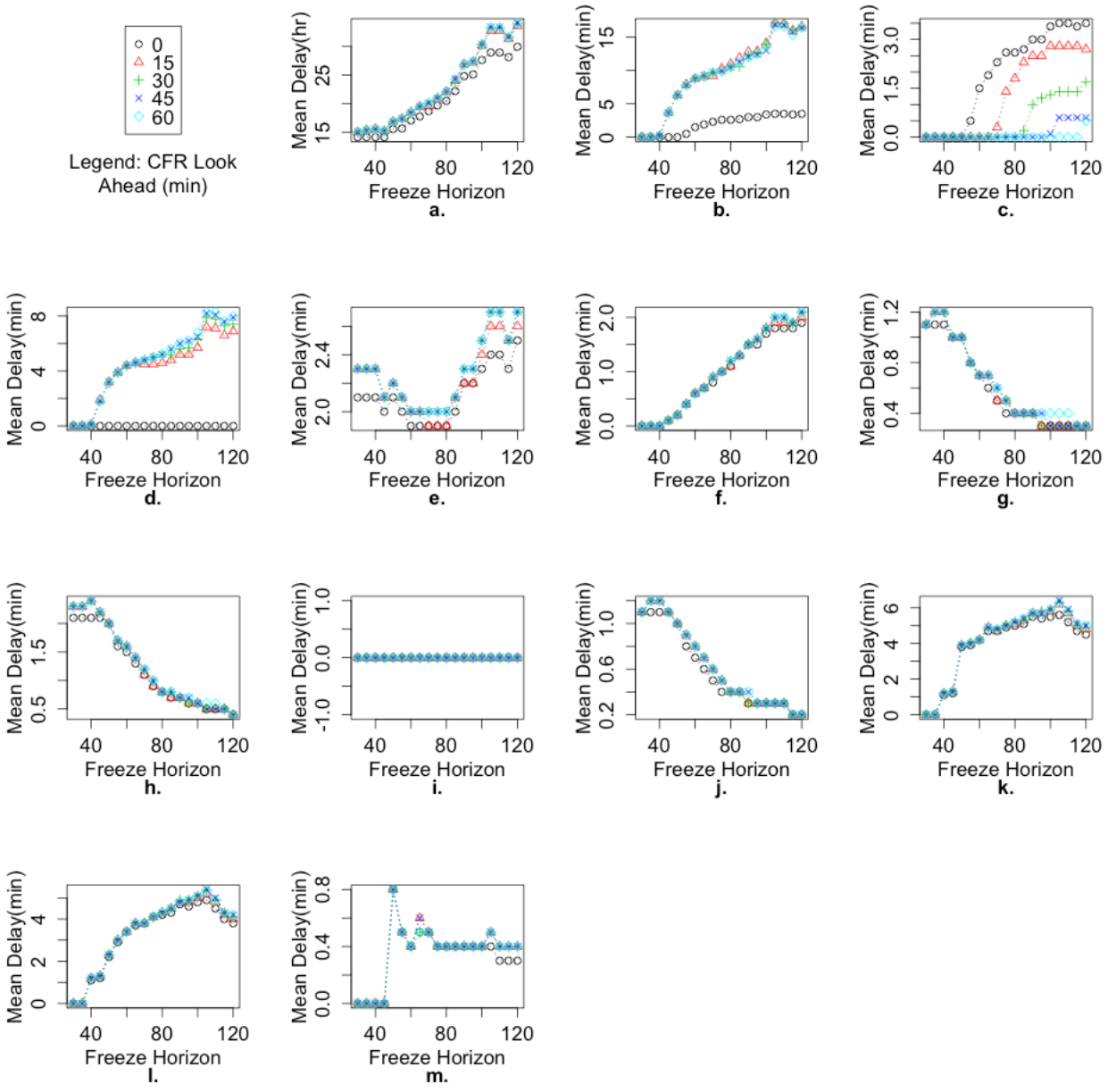

Figure 12. Results for Scenario 2a in which only DFW flights are CFR flights and wheels-off time uncertainty is not controlled.

a. system delay
b. weighted delay/CFR
c. ground delay/CFR
d. air delay/CFR
e. weighted delay/non-CFR
f. ground delay/non-CFR
g. air delay/non-CFR
h. weighted delay/non-CFR external
i. ground delay/non-CFR external
j. air delay/non-CFR external
k. weighted delay/non-CFR internal
l. ground delay/non-CFR internal
m. air delay/non-CFR internal

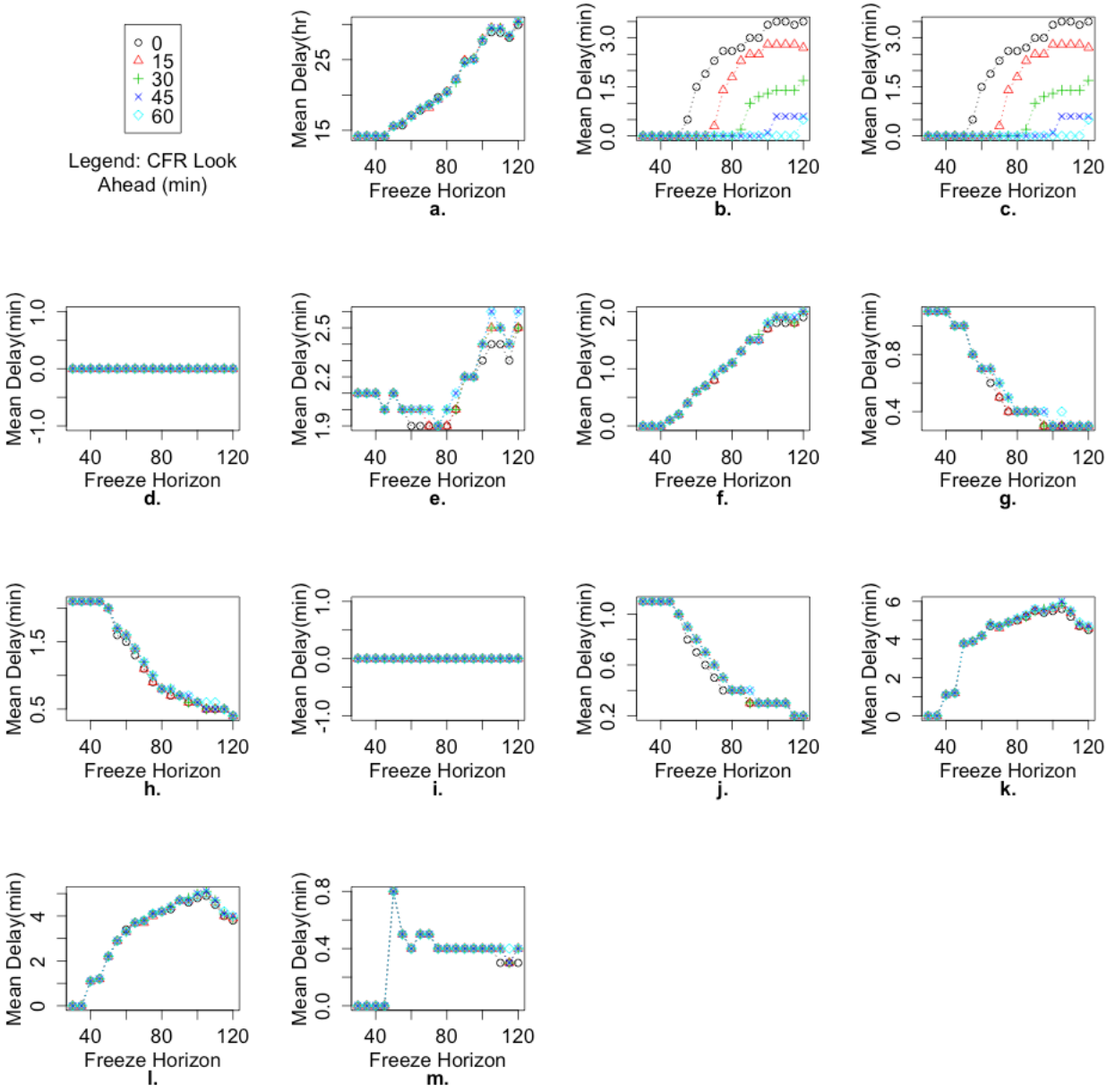

Figure 13. Results for Scenario 2b in which only DFW flights are CFR flights and wheels-off time uncertainty is controlled.

a. system delay
b. weighted delay/CFR
c. ground delay/CFR
d. air delay/CFR
e. weighted delay/non-CFR
f. ground delay/non-CFR
g. air delay/non-CFR
h. weighted delay/non-CFR external
i. ground delay/non-CFR external
j. air delay/non-CFR external
k. weighted delay/non-CFR internal
l. ground delay/non-CFR internal
m. air delay/non-CFR internal

Modeling of Gate Departure Delay and Taxi-out Delay Distributions with Normal Distributions

Earlier in Section III Subsection A, it was stated that the log of the gate departure delay and log of the taxi-out delay distributions such as the ones in Figs. 3c and 3d for the 77 ASPM airports, listed in Table 3 in this Appendix, were modeled as Gaussian distributions with mean and standard deviation values given in Table 3. It turns out that the log-delay distributions, while they appear to be symmetric, are not Gaussian distributions based on the Anderson-Darling test for normality. Given this fact, is it reasonable to model the log-delay distributions with the Gaussian distributions? This assessment was made by comparing the Probability Density Functions (PDF) and Cumulative Distribution Functions (CDF) of the log-delay distributions derived from the histograms such as the ones in Figs. 3c and 3d with those derived from analytical formulas for Gaussian distributions.

Figure 14 and 15 show the PDF and CDF of the ATL gate departure log-delay distribution and the Gaussian distribution with the same mean and standard deviation as that of the log-delay distribution. PDF for the log-delay distributions is computed from the discrete histogram as

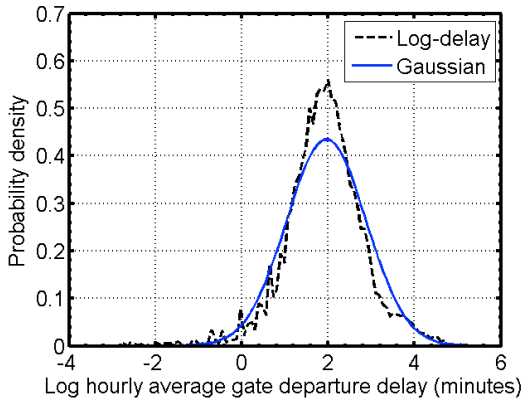

Figure 14. Comparison of ATL gate departure log-delay and Gaussian PDFs.

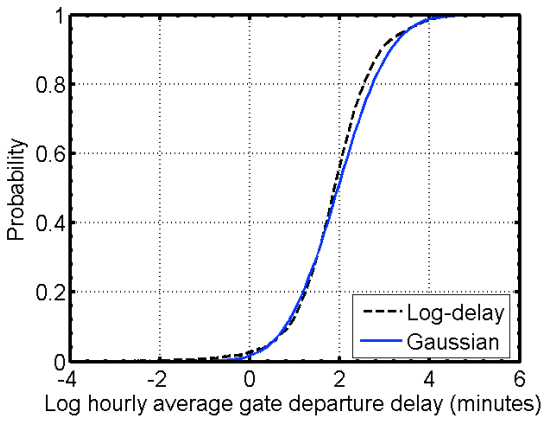

Figure 15. Comparison of ATL gate departure log-delay and Gaussian CDFs.

follows. Let n_i be the number of samples in bin i of size Δx_i of the log-delay histogram with I number of discrete bins. The probability density is then

$$f_i = \frac{n_i}{\sum_{1 \le i \le I} n_i \Delta x_i} \tag{2}$$

where f_i is the probability density associated with bin i. It follows from Eq. (2) that

$$\sum_{1 \le i \le I} f_i \Delta x_i = \frac{\sum_{1 \le i \le I} n_i \Delta x_i}{\sum_{1 \le i \le I} n_i \Delta x_i} = 1 \tag{3}$$

The probability p_i of log-delay value being less than or equal to the value represented by bin i is computed by summing the probability density up to bin i. Thus,

$$p_i = \sum_{1 \le k \le i} f_k \Delta x_k \tag{4}$$

The analytical formula for probability density for continuous Gaussian distribution is

$$f(x) = \left(\frac{1}{\sigma\sqrt{2\pi}} \right) e^{-\frac{(x-\mu)^2}{2\sigma^2}} \tag{5}$$

where μ is the mean and σ is the standard deviation. The probability of being less than or equal to x is obtained by integrating the probability density defined in Eq. (5) as follows

$$p(x) = \int_{-\infty}^{x} f(y)\,dy \tag{6}$$

It can be shown that

$$p(x) = \frac{1}{2}\left[1 + erf\left(\frac{x-\mu}{\sigma\sqrt{2}} \right) \right] \tag{7}$$

where $erf(x)$ is the error function defined as

$$erf(x) = \frac{2}{\sqrt{\pi}} \int_{0}^{x} e^{-y^2}\,dy \tag{8}$$

Figure 14 shows the probability densities computed using Eqs. (2) and (5), respectively, and Fig. 15 shows the probabilities computed using Eqs. (4) and (7), respectively. The difference of log-delay probability with respect to the Gaussian probability is shown in Fig. 16.

To improve the Gaussian distribution model of the log-delay distribution, either the standard deviation or both the mean and the standard deviation of the Gaussian distribution can be determined by either linearizing the PDF or the CDF of the Gaussian distribution and minimizing the square of the difference with respect to the log-delay distribution PDF or CDF.

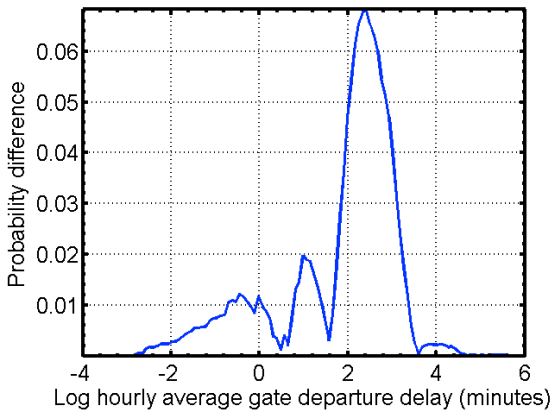

Figure 16. Absolute difference of ATL gate departure log-delay CDF with respect to Gaussian CDF.

Method I: Linearizing the PDF

Let, $\underline{\mu}$ and $\underline{\sigma}$ be the mean and the standard deviation values obtained from the log-delay distributions. Nominal probability density is obtained using Eq. (5) as

$$\underline{f}(x) = \left(\frac{1}{\underline{\sigma}\sqrt{2\pi}} \right) e^{-\frac{(x-\underline{\mu})^2}{2\underline{\sigma}^2}} \tag{9}$$

Residual (error) with respect to the probability density given by Eq. (2) is

$$df = f - \underline{f} \tag{10}$$

Rewriting Eq. (5)

$$\ln\left(\sigma\sqrt{2\pi} f\right) = -\frac{(x-\mu)^2}{2\sigma^2} \tag{11}$$

Linearizing with respect to mean and standard deviation

$$\left(\frac{\partial f}{\partial \mu}\right) d\mu + \left(\frac{\partial f}{\partial \sigma}\right) d\sigma = df \tag{12}$$

Differentiating Eq. (11), evaluating the partial derivatives about nominal mean and standard deviation values, and collecting terms, Eq. (12) can be written in the matrix notation as

$$\begin{bmatrix} \underline{f}\dfrac{(x-\underline{\mu})}{2\underline{\sigma}^2} & \underline{f}\dfrac{\left\{(x-\underline{\mu})^2 - \underline{\sigma}^2\right\}}{\underline{\sigma}^3} \end{bmatrix} \begin{bmatrix} d\mu \\ d\sigma \end{bmatrix} = df \tag{13}$$

Equation (13) is of the form

$$AX = B \tag{14}$$

Least-squares solution for the unknowns is given as

$$\begin{bmatrix} d\mu \\ d\sigma \end{bmatrix} = X = (A'A)^{-1} A'B \tag{15}$$

where A' is the transpose of matrix A and $(A'A)^{-1}$ is the inverse of $(A'A)$. The mean and standard deviation of the Gaussian distribution model can be determined as

$$\begin{aligned} \mu &= \underline{\mu} + d\mu \\ \sigma &= \underline{\sigma} + d\sigma \end{aligned} \tag{16}$$

Figures 17 and 18 show the comparison of the ATL gate departure log-delay and Gaussian PDFs and CDFs, where the Gaussian PDF and CDF are obtained with the mean and standard deviation values obtained using Eq. (16). The absolute difference of the probability of the log-delay distribution with respect to the Gaussian distribution is shown in Fig. 19. Comparing Fig. 19 to Fig. 16 it is seen that the maximum difference between the log-delay CDF and the Gaussian model CDF based on the least-squares estimates in Eq. (16) is reduced from 7% (with respect to the maximum possible difference of 1 between the two CDFs) to 3% in this example. This however was not found to be true in other examples. Keeping the mean of the

Gaussian same as the mean of the log-delay distribution and a least-squares estimate of the standard deviation (using the second term in A matrix in Eq. (14)) was found to be robust in reducing the CDF difference.

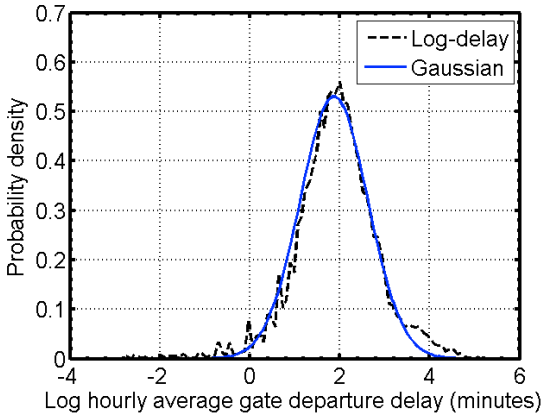

Figure 17. Comparison of ATL gate departure log-delay and Gaussian PDFs (Method I).

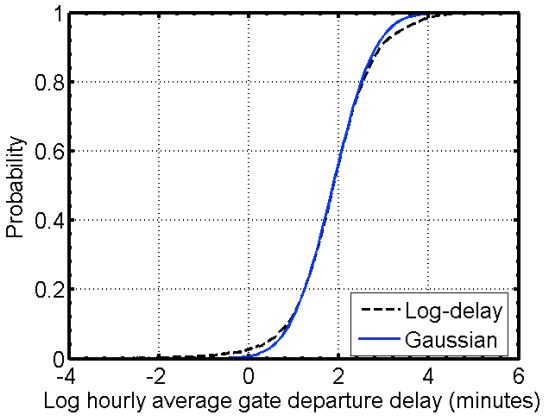

Figure 18. Comparison of ATL gate departure log-delay and Gaussian CDFs (Method I).

Since the objective is to determine the mean and the standard deviation values that minimize the difference between the CDFs of the log-delay distributions and the Gaussian distribution models, an alternative least-squares estimation can be accomplished based on linearization of the CDF in Eq. (7).

Method II: Linearizing the CDF

Let, y be a transformed variable defined as

$$y = \frac{x - \mu}{\sigma\sqrt{2}} \tag{17}$$

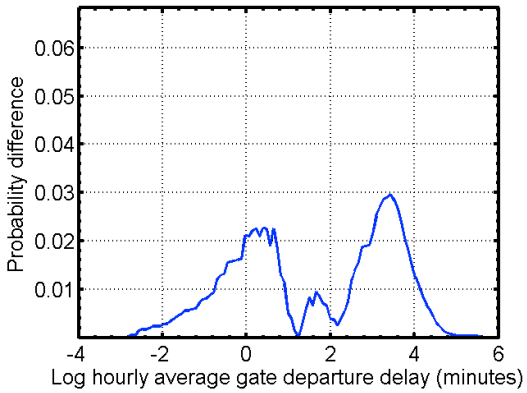

Figure 19. Absolute difference of ATL gate departure log-delay CDF with respect to Gaussian CDF (Method I).

Equation (7) can be rewritten in terms of y as follows

$$p(y) = \frac{1}{2}\left[1 + erf(y)\right] \tag{18}$$

Partial derivative of p with respect to y is obtained as

$$\frac{\partial p}{\partial y} = \frac{1}{2}\frac{\partial(erf(y))}{\partial y} = \frac{1}{\sqrt{\pi}}e^{-y^2} \tag{19}$$

Linearizing Eq. (18) with respect to the mean and the standard deviation

$$\left(\frac{\partial p}{\partial \mu}\right) d\mu + \left(\frac{\partial p}{\partial \sigma}\right) d\sigma = dp \tag{20}$$

where

$$dp = p - \underline{p} \tag{21}$$

Using Eqs. (19) and (17)

$$\frac{\partial p}{\partial \mu} = \frac{\partial p}{\partial y}\frac{\partial y}{\partial \mu} = -\frac{1}{\underline{\sigma}\sqrt{2\pi}} e^{-\left(\frac{x-\mu}{\underline{\sigma}\sqrt{2}}\right)^2} \tag{22}$$

and

$$\frac{\partial p}{\partial \sigma} = \frac{\partial p}{\partial y}\frac{\partial y}{\partial \sigma} = -\frac{(x-\mu)}{\underline{\sigma}^2\sqrt{2\pi}} e^{-\left(\frac{x-\mu}{\underline{\sigma}\sqrt{2}}\right)^2} \tag{23}$$

These two equations can be written in the form of Eq. (14) with

$$A = \left[-\frac{1}{\underline{\sigma}\sqrt{2\pi}} e^{-\left(\frac{x-\mu}{\underline{\sigma}\sqrt{2}}\right)^2} \qquad -\frac{(x-\mu)}{\underline{\sigma}^2\sqrt{2\pi}} e^{-\left(\frac{x-\mu}{\underline{\sigma}\sqrt{2}}\right)^2} \right]$$
$$B = dp \tag{24}$$
$$X = \begin{bmatrix} d\mu \\ d\sigma \end{bmatrix}$$

The least-squares solution is then obtained via Eq. (15) with the matrix and vectors defined in Eq. (24). The mean and the standard deviation values for the Gaussian model are then obtained using Eq. (16).

Figures 20 and 21 show comparisons of the ATL gate departure log-delay and Gaussian model PDFs and their CDFs, respectively, where the Gaussian model is based on the mean and standard deviation values obtained via Eqs. (24) and (16). Figure 22 shows the difference between the two CDFs in Fig. 21. Comparing Fig. 22 to Fig. 19, it is seen that the maximum of the absolute difference between the log-delay CDF and the Gaussian CDF is reduced further by 1% from 3% to 2%. The fit with respect to the PDF is a bit worse as observed comparing Fig. 20 to Fig. 17. The least-squares procedure based on CDF is the preferred procedure for both gate departure delay and taxi-out delay distributions. The revised mean and standard deviation values for the

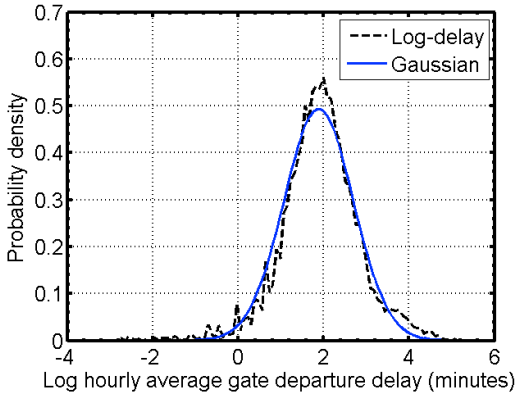

Figure 20. Comparison of ATL gate departure log-delay and Gaussian PDFs (Method II).

Gaussian models for gate departure delay and taxi-out delay for the 77 ASPM airports are listed in Table 5.

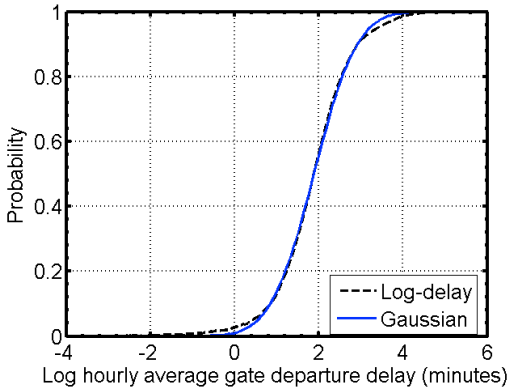

Figure 21. Comparison of ATL gate departure log-delay and Gaussian CDFs (Method II).

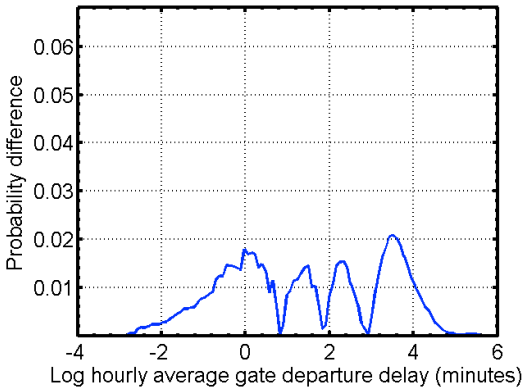

Figure 22. Absolute difference of CDFs in Fig. 21 (Method II).

While the conclusions of this report are not expected to change because of the revised mean and standard deviation values, the Gaussian distributions constructed using the values in Table 5 are closer representations of the log-delay distributions derived from the real air traffic data. In addition to the mean and standard deviation values determined using Eqs. (24) and (16), Table 5 lists the maximum absolute difference between the log-delay CDFs and the modeled Gaussian CDFs. Observe that the maximum absolute difference for gate departure delay CDFs is 6% for the 77 airports listed in Table 5. This difference for taxi-out delay is less than 10% except for Gary/Chicago International (GYY), Oxnard (OXR), Chicago Rockford International (RFD), Stewart International (SWF), Teterboro (TEB) and Van Nuys (VNY); values for these six airports are marked in red. The number of samples for constructing Gaussians for these airports were small in comparison to the 8,727 samples for Atlanta, mentioned earlier in Section III Subsection A. GYY, OXR, RFD, SWF, TEB and VNY had 65, 176, 306, 1245, 1239 and 498 samples, respectively, in the 2011 data derived from FAA's ASPM database employed in this report. These samples should be augmented with samples from other years from the ASPM database to construct reliable Gaussians for modeling taxi-out log-delay distributions for these airports.

Table 5. Hourly average gate departure and taxi-out log-delay Gaussian models

Airport Code	Hourly Average Gate Departure Delay			Hourly Average Taxi-out Delay		
	Mean	Standard Deviation	Maximum Absolute CDF error (%)	Mean	Standard Deviation	Maximum Absolute CDF error (%)
ABQ	1.407	1.186	3	0.517	0.898	4
ANC	1.430	1.015	4	-0.082	1.416	6
ATL	1.884	0.809	2	1.612	0.636	4
AUS	1.670	1.096	4	0.204	0.920	6
BDL	1.718	1.160	3	0.377	1.103	5
BHM	1.820	1.289	3	0.390	1.086	3
BNA	1.682	1.059	4	0.438	0.858	4
BOS	1.835	0.900	2	1.168	0.756	2
BUF	1.938	1.208	4	0.189	1.280	1
BUR	1.506	1.286	4	0.304	0.859	3
BWI	1.812	0.985	3	0.681	0.786	2
CLE	1.713	1.040	3	0.556	1.036	2
CLT	1.870	0.806	3	1.387	0.663	3
CVG	1.830	1.055	3	0.084	1.222	2
DAL	1.971	0.931	3	0.017	0.898	6
DAY	1.706	1.348	3	0.444	1.199	3
DCA	1.623	0.929	2	1.000	0.804	3
DEN	1.828	0.847	3	0.708	0.751	5
DFW	1.949	0.685	3	0.835	0.483	3
DTW	1.938	0.816	3	0.514	0.951	3
EWR	2.099	0.922	2	1.569	0.852	1
FLL	1.784	0.922	3	0.918	0.783	2
GYY	3.034	0.951	4	-0.384	0.008	11
HNL	1.078	0.993	4	0.268	0.814	4
HOU	1.943	0.953	4	0.098	0.898	3
HPN	2.611	0.847	4	0.223	1.292	5
IAD	2.186	0.841	3	0.596	1.002	4
IAH	1.833	0.726	3	1.090	0.688	3
IND	1.823	1.104	3	-0.005	1.102	3
ISP	1.779	1.473	5	-0.055	1.070	4
JAX	1.530	1.280	3	0.363	0.974	4
JFK	2.080	0.869	2	1.284	1.124	1
LAS	1.731	0.740	4	0.971	0.615	3
LAX	1.796	0.667	2	1.060	0.569	3
LGA	1.887	0.955	2	1.922	0.947	2
LGB	1.630	1.336	3	0.454	1.136	3

Table 5. Hourly average gate departure and taxi-out log-delay Gaussian models (contd.)

Airport Code	Hourly Average Gate Departure Delay			Hourly Average Taxi-out Delay		
	Mean	Standard Deviation	Maximum Absolute CDF error (%)	Mean	Standard Deviation	Maximum Absolute CDF error (%)
MCI	1.633	1.058	3	0.281	0.949	3
MCO	1.633	0.963	3	0.961	0.622	3
MDW	2.052	0.849	3	0.616	0.808	3
MEM	2.115	1.045	3	0.330	1.120	5
MHT	2.000	1.345	3	-0.050	1.317	4
MIA	2.282	0.705	3	0.863	0.639	3
MKE	1.849	1.106	2	0.286	1.041	3
MSP	1.744	0.860	3	0.706	0.878	2
MSY	1.463	1.245	4	0.316	0.924	4
OAK	1.761	1.001	4	-0.026	1.052	5
OGG	0.998	1.188	4	-0.002	0.951	3
OMA	1.699	1.153	4	0.147	1.150	2
ONT	1.697	1.461	2	0.070	1.134	4
ORD	1.973	0.844	2	1.200	0.705	3
OXR	2.989	0.999	4	1.153	0.230	**22**
PBI	2.190	1.052	4	0.328	0.953	4
PDX	1.398	1.045	3	0.448	0.772	5
PHL	1.993	0.925	2	1.164	1.115	1
PHX	1.569	0.778	3	0.845	0.768	2
PIT	1.845	1.071	3	0.323	1.144	2
PSP	2.039	1.210	5	0.675	0.990	4
PVD	1.858	1.239	4	0.397	1.174	2
RDU	1.888	1.056	3	0.748	0.842	4
RFD	2.414	1.315	6	-0.550	0.240	**18**
RSW	1.512	1.258	4	0.325	0.974	3
SAN	1.465	0.993	3	0.682	0.747	2
SAT	1.573	1.108	4	0.582	0.750	5
SDF	1.953	1.187	4	-0.036	1.239	3
SEA	1.258	0.893	3	0.553	0.724	3
SFO	1.803	0.863	2	1.143	0.607	2
SJC	1.453	1.131	4	0.191	0.852	3
SJU	1.573	1.179	3	0.211	0.979	4
SLC	1.452	0.981	3	1.005	0.846	4
SMF	1.356	1.156	3	0.309	0.843	3
SNA	1.496	1.106	4	0.367	1.028	4
STL	1.779	0.946	4	0.112	0.850	3

Table 5. Hourly average gate departure and taxi-out log-delay Gaussian models (contd.)

Airport Code	Hourly Average Gate Departure Delay			Hourly Average Taxi-out Delay		
	Mean	Standard Deviation	Maximum Absolute CDF error (%)	Mean	Standard Deviation	Maximum Absolute CDF error (%)
SWF	2.631	1.285	4	0.165	1.629	**10**
TEB	3.294	0.671	5	-0.664	0.182	**16**
TPA	1.374	1.240	3	0.411	0.769	3
TUS	1.343	1.309	4	0.562	0.942	4
VNY	3.280	0.790	4	-0.545	0.045	**14**

REFERENCES

1. Engelland, S., and Capps, A., "Trajectory-Based Takeoff Time Predictions Applied to Tactical Departure Scheduling: Concept Description, System Design, and Initial Observations," AIAA-2011-6875, *Proceedings of 11th AIAA Aviation Technology, Integration, and Operations (ATIO) Conference*, Virginia Beach, Virginia, Sep. 20-22, 2011.
2. Palopo, K., Chatterji, G. B., and Almog, N., "Delay Sensitivity to Call For Release Scheduling Time," AIAA-2012-5698, *Proceedings of 12th AIAA Aviation Technology, Integration, and Operations (ATIO) Conference*, Indianapolis, Indiana, Sep. 17-19, 2012.
3. Wong, G. L., "The Dynamic Planner: The Sequencer, Scheduler, and Runway Allocator for Air Traffic Control Automation," NASA TM-2000-209586, National Aeronautics and Space Administration, Ames Research Center, Moffett Field, CA 94035-1000, April 2000, URL: http://www.aviationsystemsdivision.arc.nasa.gov/publications/full_list_by_author.shtml [cited: 11/6/2013].
4. "Boeing 777," Wikipedia, URL: https://en.wikipedia.org/wiki/Boeing_777 [cited: 08/15/2016].
5. "Final Year 2 Report for the Traffic Flow Management Validation Techniques Project," Document No.: 201214582-D05, Version: 1, Contract: NNA11AA45C, Prepared for: NASA Ames Research Center, Moffett Field, CA 94035, Saab Sensis Corporation, 85 Collamer Crossings, East Syracuse, New York 13057, Sep. 12, 2012.
6. Meyn, L., Windhorst, R., Roth, K., Drei, D. V., Kubat, G., Manikonda, V., Roney, S., Hunter, G., Huang, A., and Couluris, G., "Build 4 of the Airspace Concept Evaluation System," *Proceedings of the AIAA Modeling and Simulation Technologies Conference and Exhibit*, Keystone, Colorado, Aug. 21-24, 2006.
7. "User Manual for Base of Aircraft Data (BADA) Revision 3.6," Eec note no. 10/04, Eurocontrol Experimental Centre, July 2004.
8. Zelinski, S. J., "Validating the Airspace Concept Evaluation System Using Real World Data," *Proceedings of the AIAA Modeling and Simulation Technologies Conference and Exhibit*, San Francisco, California, Aug. 15-18, 2005.
9. Zelinski, S. J., and Meyn, L., "Validating the Airspace Concept Evaluation System for Different Weather Days," *Proceedings of the AIAA Modeling and Simulation Technologies Conference and Exhibit*, Keystone, Colorado, Aug. 21-24, 2006.